NASA Contractor Report 198538

A Method for Generating Reduced Order Linear Models of Supersonic Inlets

Amy Chicatelli and Tom T. Hartley
University of Akron
Akron, Ohio

January 1997

Prepared for
Lewis Research Center
Under Grant NAG3–1450

National Aeronautics and
Space Administration

Contents

A Method for Generating Reduced Order Linear Models of Supersonic Inlets

Amy Chicatelli
Tom T. Hartley

The Department of Electrical Engineering
University Of Akron
Akron, OH 44325-3904

Summary

Simulation of high speed propulsion systems may be divided into two categories, nonlinear and linear. The nonlinear simulations include simulations based on computational fluid dynamics (CFD) methodologies. These simulations tend to provide high resolution results that show the fine detail of the flow. Consequently, the simulations are large, numerically intensive, and run much slower than real-time. Linear models are generally used during the preliminary stages of control design. These simplistic models often run at or near real-time but do not always capture the detailed dynamics of the plant. Under a grant sponsored by the NASA Lewis Research Center, Cleveland, Ohio, a new method has been developed that can be used to generate improved linear models for control design from steady-state CFD results. This method provides a small perturbation model that can be used for control applications and real-time simulations. It is important to note the utility of the modeling procedure; all that is needed to obtain a linear model of the propulsion system is the spatial step and steady-state operating conditions from a CFD simulation or experiment. This research represents a beginning step in establishing a bridge between the controls discipline and the CFD discipline so that the control engineer is able to effectively use CFD results in control system design and analysis.

1 Introduction

The development of inlet models for high speed propulsion systems is important because of the current interest in high speed air-breathing propulsion systems, such as the High Speed Civil Transport (HSCT) and the High Speed Research (HSR) project. Modeling of these systems is difficult because of their complex physical processes which are represented by nonlinear partial differential equations (PDE). Without a good model the control engineer cannot develop a good control design. To design these control systems, an adequate model of the entire system or particular subsystem is necessary; typically these models are either based on traditional propulsion control models or CFD models.

Traditional propulsion control models typically utilize a large lumping technique for the spatial derivatives so that the propulsion system is represented by a set of nonlinear ordinary differential equations (ODE). These equations are often linearized about a steady-state point so that the control model is linear. Methods based on this linear ODE approach have been developed for propulsion systems, some of which are: the Cole-Willoh model [1], the Martin model [2], the Barry models [3], circuit models [4], and the Laplace transform of the Green's function method [5] [6]. Unfortunately these models are often difficult to implement and do not always capture the nonlinear dynamics of the system.

Accurate nonlinear models of complex flows are usually obtained from CFD codes [7] [8]. These models can to some degree predict the behavior of large perturbations in the flow field, including unstart, buzz, turbulence, boundary layer growth, etc.. Typically these CFD models are based on a large number of nodes which can then be used in a finite difference method to produce a large system of nonlinear equations. However due to their nonlinearity and large size, these models require large amounts of computer time and therefore are not suitable for controls analysis and design.

An effective propulsion system model for control system design must adequately capture the dynamics of the system but also be of small order. CFD models fulfill the first requirement, and traditional models fulfill the second requirement. Therefore, a method that is based on both ideas might provide a reasonable model for controls applications. This paper develops a method for the direct use of a linearized CFD method combined with model reduction to model the internal flow of a propulsion system.

In this paper, the quasi-one-dimensional inviscid flow of an axisymmetric inlet is the propulsion system of primary interest. The next section describes the CFD model development which is the basis for the linear model of the inlet; this includes the governing equations, the development of the split flux model, and the development of the boundary conditions. Then in section three, the linear model is derived by implementing linearized methods of the previous section; various inputs and outputs are also developed in this section. A summary of the model reduction method and calculation of the associated error bounds follow in sections four and five. In section six, an application of the method is illustrated on a mixed compression axisymmetric inlet for a variety of inputs and outputs, and a conclusion follows in section seven.

2 CFD Model Development

2.1 Governing Equations

The dynamics of an internal flow propulsion system are often represented by the nonviscous quasi-one-dimensional Euler equations. The conservative form of these equations is defined by Hirsch [9] as:

Conservation of Mass:

$$\frac{\partial(\rho A)}{\partial t} + \frac{\partial(\rho u A)}{\partial x} = 0 \tag{2.1}$$

Conservation of Momentum:

$$\frac{\partial(\rho u A)}{\partial t} + \frac{\partial\left(\rho u^2 + p\right) A}{\partial x} = p\frac{\partial A}{\partial x} \tag{2.2}$$

Conservation of Energy:

$$\frac{\partial(\rho E A)}{\partial t} + \frac{\partial(\rho u H A)}{\partial x} = 0 \tag{2.3}$$

where $H = \left(E + \frac{p}{\rho}\right)$ and A represents the cross-sectional area. If the partial derivative terms are expanded,

the area terms can be extracted and the conservative form of the equations can be rewritten as:

$$\frac{\partial \vec{u}}{\partial t} + \frac{\partial F(\vec{u})}{\partial x} = G(\vec{u}) \tag{2.4}$$

where the vector components, $\vec{u}$, $F(\vec{u})$, and $G(\vec{u})$, are defined below.

State vector:

$$\vec{u} = \begin{bmatrix} \rho \\ \rho u \\ \rho E \end{bmatrix} = \begin{bmatrix} \rho \\ m \\ \varepsilon \end{bmatrix} \tag{2.5}$$

ε is defined as, $\varepsilon = \rho E = \rho\left(e + \frac{u^2}{2}\right)$, and e is the internal energy per unit mass.

Flux vector:

$$F(\vec{u}) = \begin{bmatrix} \rho u \\ \rho u^2 + p \\ u(\varepsilon + p) \end{bmatrix} \tag{2.6}$$

Source vector:

$$G(\vec{u}) = \begin{bmatrix} -\frac{1}{A}\left\{\rho\frac{\partial A}{\partial t} + \rho u\frac{\partial A}{\partial x}\right\} \\ -\frac{1}{A}\left\{\rho u\frac{\partial A}{\partial t} + \rho u^2\frac{\partial A}{\partial x}\right\} \\ -\frac{1}{A}\left\{\varepsilon\frac{\partial A}{\partial t} + u(\varepsilon + p)\frac{\partial A}{\partial x}\right\} \end{bmatrix} \tag{2.7}$$

If the cross-sectional area, A, does not vary with time, then the $\frac{\partial A}{\partial t}$ terms may be eliminated from the source vector. For a perfect gas, the pressure can be defined as $p = (\gamma - 1)\left(\varepsilon - \frac{m^2}{2\rho}\right)$, and the flux vector may be rewritten in the following variables.

$$F(\vec{u}) = \begin{bmatrix} m \\ (\gamma - 1)\varepsilon + (3 - \gamma)\frac{m^2}{2\rho} \\ \frac{\gamma \varepsilon m}{\rho} - (\gamma - 1)\frac{m^3}{2\rho^2} \end{bmatrix} \tag{2.8}$$

The derivative of the flux vector with respect to x can be represented in quasi-linear form by replacing $\frac{\partial F(\vec{u})}{\partial x}$ with $J\frac{\partial \vec{u}}{\partial x}$, where J is the Jacobian of the flux vector and defined below.

$$J = \frac{\partial F(\vec{u})}{\partial \vec{u}} = \begin{bmatrix} 0 & 1 & 0 \\ \frac{1}{2}(\gamma - 3)\left(\frac{m}{\rho}\right)^2 & (3 - \gamma)\frac{m}{\rho} & \gamma - 1 \\ \left\{(\gamma - 1)\left(\frac{m}{\rho}\right)^3 - \frac{\gamma \varepsilon m}{\rho^2}\right\} & \left\{\frac{\gamma \varepsilon}{\rho} - \frac{3}{2}(\gamma - 1)\left(\frac{m}{\rho}\right)^2\right\} & \frac{\gamma m}{\rho} \end{bmatrix} \tag{2.9}$$

The substitution of (2.9) into equation (2.4) results in the following partial differential equation,

$$\frac{\partial \vec{u}}{\partial t} + J\frac{\partial \vec{u}}{\partial x} = G(\vec{u}) \tag{2.10}$$

The characteristics, or local eigenvalues, of the Jacobian are equal to:

$$\begin{aligned} \lambda_1 &= u \\ \lambda_2 &= u + c \\ \lambda_3 &= u - c \end{aligned} \tag{2.11}$$

Equation (2.10) can be transformed into a system of ordinary differential equations by replacing the spatial derivative term with a finite difference expression; then the system of equations may be integrated numerically to obtain the flow field solution. In order for the overall system to be numerically stable, the direction of the characteristics (2.11) must be taken into account when the spatial derivative is replaced. When the flow is supersonic, the characteristics are all positive, and one finite difference expression can be used for the $\frac{\partial \vec{u}}{\partial x}$ term. If the flow is subsonic, the signs of the characteristics are mixed, and a single finite difference expression for $\frac{\partial \vec{u}}{\partial x}$ will create an unstable model. If equation (2.10) is divided according to the sign of the characteristics, then a different finite difference expression for the spatial derivative can be used for each of the positive and negative terms. The next section illustrates how to split the system into its positive and negative parts.

2.2 Split Flux Model

The split flux method detailed in references [9] and [10] is summarized in this section. The split flux method separates the flux vector into subvectors which correspond to the positive and negative characteristics of the Jacobian. The split flux model can be written as the following equation,

$$\frac{\partial \vec{u}}{\partial t} + \frac{\partial F^+(\vec{u})}{\partial x} + \frac{\partial F^-(\vec{u})}{\partial x} = G(\vec{u}) \tag{2.12}$$

Since $F(\vec{u})$ is a homogenous function of degree one in $\vec{u}$, it can be written as:

$$F(\vec{u}) = J\vec{u} \tag{2.13}$$

and the positive and negative subvectors can be calculated from the following:

$$F^{\pm}(\vec{u}) = J^{\pm}\vec{u} \tag{2.14}$$

Substitution of equation (2.14) into the split flux model equation (2.12) produces the following result.

$$\frac{\partial \vec{u}}{\partial t} + J^+\frac{\partial \vec{u}}{\partial x} + J^-\frac{\partial \vec{u}}{\partial x} = G(\vec{u}) \tag{2.15}$$

The positive and negative Jacobians satisfy $J = J^+ + J^-$ and are calculated from:

$$J^{\pm} = K\Lambda^{\pm}K^{-1} \tag{2.16}$$

The right eigenvectors of J are defined as:

$$K = \begin{bmatrix} 1 & \rho c & -\rho c \\ u & \frac{\rho}{2c}(u+c) & -\frac{\rho}{2c}(u-c) \\ \frac{u^2}{2} & \frac{\rho}{2c}\left(\frac{u^2}{2} + uc + \frac{c^2}{\gamma-1}\right) & -\frac{\rho}{2c}\left(\frac{u^2}{2} - uc + \frac{c^2}{\gamma-1}\right) \end{bmatrix} \tag{2.17}$$

and the matrices Λ^+ and Λ^- can be defined as:

$$\Lambda^{\pm} = \begin{bmatrix} \frac{1}{2}(u \pm |u|) & 0 & 0 \\ 0 & \frac{1}{2}(u+c \pm |u+c|) & 0 \\ 0 & 0 & \frac{1}{2}(u-c \pm |u-c|) \end{bmatrix} \tag{2.18}$$

There are a variety of splittings that can be used for Λ. As long as the characteristics of Λ^+ and Λ^- satisfy $\Lambda = \Lambda^+ + \Lambda^-$, the splitting is valid. Once the system, equation (2.15), is split into its positive and negative Jacobians, a different finite difference expression can be used to approximate $\frac{\partial \vec{u}}{\partial x}$ for each Jacobian. The spatial derivative associated with the positive Jacobian is discretized with a backward difference operator:

$$\frac{\partial \vec{u}_i}{\partial x} = \frac{\vec{u}_i - \vec{u}_{i-1}}{\Delta x_i} \tag{2.19}$$

and the spatial derivative associated with the negative Jacobian is discretized with a forward difference operator:

$$\frac{\partial \vec{u}_i}{\partial x} = \frac{\vec{u}_{i+1} - \vec{u}_i}{\Delta x_i} \tag{2.20}$$

Δx_i denotes the spatial step and i denotes the grid point. The above substitutions are put into equation (2.15) which results in the following equation for each grid point of the system.

$$\frac{\partial \vec{u}_i}{\partial t} + J_i^+ \left(\frac{\vec{u}_i - \vec{u}_{i-1}}{\Delta x_i} \right) + J_i^- \left(\frac{\vec{u}_{i+1} - \vec{u}_i}{\Delta x_i} \right) = G(\vec{u}_i) \tag{2.21}$$

This can be simplified and rewritten as:

$$\frac{\partial \vec{u}_i}{\partial t} - J_i^+ \frac{\vec{u}_{i-1}}{\Delta x_i} + \left(J_i^+ - J_i^- \right) \frac{\vec{u}_i}{\Delta x_i} + J_i^- \frac{\vec{u}_{i+1}}{\Delta x_i} = G(\vec{u}_i) \tag{2.22}$$

Equation (2.22) represents the dynamics of the internal grid points of the CFD model; there are still boundary conditions at the cowl lip and compressor face that must be satisfied. These boundary conditions are developed in the next section.

2.3 Boundary Conditions

Boundary conditions are required at the cowl lip and compressor face of the inlet CFD model, because the finite difference expressions at these grid points have terms which lie outside of the computational domain. Boundary conditions can be categorized as either physical or numerical. Numerical boundary conditions correspond to characteristics leaving the domain, and physical boundary conditions correspond to characteristics entering the domain. Therefore the numerical boundary conditions can be determined from the interior grid points of the computational domain, but the physical boundary conditions must be specified. There are a variety of methods that can be used for the treatment of the boundary conditions; compatibility relations with time-differenced physical boundary conditions is the one implemented here from Hirsch [9]. With this method, the incoming characteristics are set equal to zero so that only information transmitted from the interior is maintained. The general development for the treatment of the boundary conditions as taken from [9] follows.

If the governing PDE, equation (2.4) from section 2.1,

$$\frac{\partial \vec{u}}{\partial t} + \frac{\partial F(\vec{u})}{\partial x} = G(\vec{u})$$

is rewritten in terms of the characteristic variables for the time derivative, the incoming characteristics can be replaced by the physical boundary conditions. Equation (2.23) shows the characteristic variables, $\overrightarrow{w}$,

$$\overrightarrow{w} = \begin{bmatrix} s \\ u + \frac{2}{\gamma - 1}c \\ u - \frac{2}{\gamma - 1}c \end{bmatrix} \tag{2.23}$$

and equation (2.24) shows the transformation between the conservative variables, $\overrightarrow{u}$, and the characteristic variables.

$$\frac{\partial \overrightarrow{u}}{\partial t} = K \frac{\partial \overrightarrow{w}}{\partial t} \tag{2.24}$$

The result of applying transformation (2.24) to equation (2.10) is shown in the equation below.

$$\begin{aligned} K\frac{\partial \overrightarrow{w}}{\partial t} + J\frac{\partial \overrightarrow{u}}{\partial x} &= G(\overrightarrow{u}) \\ \frac{\partial \overrightarrow{w}}{\partial t} + K^{-1}J\frac{\partial \overrightarrow{u}}{\partial x} &= K^{-1}G(\overrightarrow{u}) \end{aligned} \tag{2.25}$$

Now the characteristic variables can be split into the incoming physical characteristics, $\overrightarrow{w}^P$, and the outgoing numerical characteristics, $\overrightarrow{w}^N$.

$$\frac{\partial}{\partial t}\begin{bmatrix} \overrightarrow{w}^P \\ \overrightarrow{w}^N \end{bmatrix} + \begin{bmatrix} (K^{-1})^P \\ (K^{-1})^N \end{bmatrix} J\frac{\partial \overrightarrow{u}}{\partial x} = \begin{bmatrix} (K^{-1})^P \\ (K^{-1})^N \end{bmatrix} G(\overrightarrow{u}) \tag{2.26}$$

The partitioning of the K matrix shown here will be discussed in Section 3.3.1. With this boundary condition method, information transmitted by the characteristics to the interior is discarded. Therefore, the incoming characteristics are set equal to zero by replacing them with the physical boundary condition, $B_{bc} = 0$, as shown in equation (2.27).

$$\frac{\partial}{\partial t}\begin{bmatrix} B_{bc} \\ \overrightarrow{w}^N \end{bmatrix} + \begin{bmatrix} 0 \\ (K^{-1})^N \end{bmatrix} J\frac{\partial \overrightarrow{u}}{\partial x} = \begin{bmatrix} 0 \\ (K^{-1})^N \end{bmatrix} G(\overrightarrow{u}) \tag{2.27}$$

Converting back to conservative variables and replacing $\frac{\partial B_{bc}}{\partial t}$ with $\frac{\partial B_{bc}}{\partial \overrightarrow{u}}\frac{\partial \overrightarrow{u}}{\partial t}$ yields,

$$\begin{bmatrix} \frac{\partial B_{bc}}{\partial \overrightarrow{u}}\frac{\partial \overrightarrow{u}}{\partial t} \\ (K^{-1})^N \frac{\partial \overrightarrow{u}}{\partial t} \end{bmatrix} + \begin{bmatrix} 0 \\ (K^{-1})^N \end{bmatrix} J\frac{\partial \overrightarrow{u}}{\partial x} = \begin{bmatrix} 0 \\ (K^{-1})^N \end{bmatrix} G(\overrightarrow{u}) \tag{2.28}$$

Now the implementation of the time-differenced boundary condition is performed; this is done by taking the derivative of B_{bc} with respect to time.

$$\begin{aligned} \frac{\partial B_{bc}}{\partial t} &= \frac{\partial B_{bc}}{\partial \overrightarrow{u}}\frac{\partial \overrightarrow{u}}{\partial t} \\ B_{bc}\left(\overrightarrow{u}^{n+1}\right) - B_{bc}\left(\overrightarrow{u}^{n}\right) &= \frac{\partial B_{bc}}{\partial \overrightarrow{u}}\left(\overrightarrow{u}^{n+1} - \overrightarrow{u}^{n}\right) \\ B_{bc}\left(\overrightarrow{u}^{n+1}\right) &= B_{bc}\left(\overrightarrow{u}^{n}\right) + \frac{\partial B_{bc}}{\partial \overrightarrow{u}}\left(\overrightarrow{u}^{n+1} - \overrightarrow{u}^{n}\right) \end{aligned} \tag{2.29}$$

Now $B_{bc}\left(\overrightarrow{u}^{n+1}\right)$ is set equal to zero, because it has replaced the incoming characteristic.

$$\begin{aligned} 0 &= B_{bc}\left(\overrightarrow{u}^{n}\right) + \frac{\partial B_{bc}}{\partial \overrightarrow{u}}\left(\overrightarrow{u}^{n+1} - \overrightarrow{u}^{n}\right) \\ -B_{bc}\left(\overrightarrow{u}^{n}\right) &= \frac{\partial B_{bc}}{\partial \overrightarrow{u}}\left(\overrightarrow{u}^{n+1} - \overrightarrow{u}^{n}\right) \\ -B_{bc}\left(\overrightarrow{u}^{n}\right) &= \frac{\partial B_{bc}}{\partial \overrightarrow{u}}\frac{\partial \overrightarrow{u}}{\partial t} \end{aligned} \tag{2.30}$$

Substitute the last line of (2.30) into equation (2.28).

$$\begin{bmatrix} \frac{\partial B_{bc}}{\partial \overrightarrow{u}} \\ \left(K^{-1}\right)^{N} \end{bmatrix} \frac{\partial \overrightarrow{u}}{\partial t} + \begin{bmatrix} 0 \\ \left(K^{-1}\right)^{N} \end{bmatrix} J\frac{\partial \overrightarrow{u}}{\partial x} = \begin{bmatrix} -B_{bc} \\ \left(K^{-1}\right)^{N} G\left(\overrightarrow{u}\right) \end{bmatrix} \tag{2.31}$$

Let K_1 be defined as:

$$K_1 = \begin{bmatrix} \frac{\partial B_{bc}}{\partial \overrightarrow{u}} \\ \left(K^{-1}\right)^{N} \end{bmatrix} \tag{2.32}$$

and K_2 be defined as:

$$K_2 = \begin{bmatrix} 0 \\ \left(K^{-1}\right)^{N} \end{bmatrix} \tag{2.33}$$

Substitute (2.32) and (2.33) into equation (2.31) and simplify.

$$\frac{\partial \overrightarrow{u}}{\partial t} + K_1^{-1}K_2 J\frac{\partial \overrightarrow{u}}{\partial x} = K_1^{-1}\begin{bmatrix} -B_{bc} \\ \left(K^{-1}\right)^{N} G\left(\overrightarrow{u}\right) \end{bmatrix} \tag{2.34}$$

This is the boundary equation used at the cowl lip and compressor face. Since the incoming characteristics have been zeroed out and replaced with physical boundary conditions, the spatial derivative can be replaced with one finite difference expression. At the cowl lip the spatial derivative is replaced with a forward difference equation (2.20), and at the compressor face the spatial derivative is replaced with a backward difference equation (2.19). The next section develops the linear model using the split flux technique from section 2.2 and the boundary condition method from this section.

3 Linear Model Development

3.1 Small Perturbation Model

For a small perturbation model, the states, inputs, and outputs of a nonlinear system are assumed to be the combination of a steady-state value and a small time dependent perturbation as shown in equations (3.1) through (3.3) below.

States:

$$\overrightarrow{X} = \overrightarrow{X}_{ss} + \delta\overrightarrow{X} \tag{3.1}$$

Inputs:

$$\overrightarrow{U} = \overrightarrow{U}_{ss} + \delta\overrightarrow{U} \tag{3.2}$$

Outputs:

$$\vec{Y} = \vec{Y}_{ss} + \delta\vec{Y} \tag{3.3}$$

The small perturbation model is only valid when operating within a small region around the steady-state value; once outside this region, the linear model is no longer an accurate representation of the nonlinear system. In other words, the farther the nonlinear model moves away from the operating point, the less accurate the linear dynamic response.

In general the small perturbation model will have as many grid points as the CFD model. Because of the large number of equations in the CFD based model, it is convenient to describe the small perturbation model in state space format; this also facilitates the placement of the inputs and outputs for the system.

$$\begin{aligned} \frac{d}{dt}\delta\vec{X} &= \mathbf{A}\delta\vec{X} + \mathbf{B}\delta\vec{U} \\ \delta\vec{Y} &= \mathbf{C}\delta\vec{X} + \mathbf{D}\delta\vec{U} \end{aligned} \tag{3.4}$$

The A, B, C, and D matrices are defined as follows:

$$\begin{aligned} \mathbf{A} &= \textit{system matrix} \\ \mathbf{B} &= \textit{input matrix} \\ \mathbf{C} &= \textit{output matrix} \\ \mathbf{D} &= \textit{input/output matrix} \end{aligned} \tag{3.5}$$

The data needed for the calculation of these matrices is obtained from a steady-state operating point of the propulsion system model. Contents of these matrices are developed in the following sections.

3.2 System Matrix

The system matrix for the small perturbation model is generated by applying equation (2.22) to each grid point of the propulsion system with the Jacobian evaluated at a steady-state operating point. The source vector may then be rewritten in quasilinear form, $G(\vec{u}) = J_S\vec{u}$, and evaluated at the same operating point. The Jacobian of the area source vector is shown below.

$$J_S = \frac{\partial G(\vec{u})}{\partial \vec{u}} = \begin{bmatrix} 0 & -\left(\frac{1}{A}\right)\frac{\partial A}{\partial x} & 0 \\ \left(\frac{m^2}{\rho^2 A}\right)\frac{\partial A}{\partial x} & -\left(\frac{2m}{\rho A}\right)\frac{\partial A}{\partial x} & 0 \\ \left\{-(\gamma-1)\left(\frac{m}{\rho}\right)^3 + \frac{\gamma\varepsilon m}{\rho^2}\right\}\frac{1}{A}\frac{\partial A}{\partial x} & \left\{-\frac{\gamma\varepsilon}{\rho} + \frac{3}{2}(\gamma-1)\left(\frac{m}{\rho}\right)^2\right\}\frac{1}{A}\frac{\partial A}{\partial x} & -\left(\frac{\gamma m}{\rho A}\right)\frac{\partial A}{\partial x} \end{bmatrix} \tag{3.6}$$

With the above definition, equation (2.22) becomes:

$$\frac{\partial \delta\vec{u}_i}{\partial t} - J_i^+\frac{\delta\vec{u}_{i-1}}{\Delta x_i} + \left(J_i^+ - J_i^-\right)\frac{\delta\vec{u}_i}{\Delta x_i} + J_i^-\frac{\delta\vec{u}_{i+1}}{\Delta x_i} = J_{S_i}\delta\vec{u}_i \tag{3.7}$$

Equation (3.7) can be written in the following compact form:

$$\frac{d}{dt}\delta\vec{X} = \mathbf{A}\delta\vec{X} \tag{3.8}$$

with $\delta\overrightarrow{X}$ defined as:

$$\delta\overrightarrow{X} = \begin{bmatrix} \delta\overrightarrow{u}_1 \\ \delta\overrightarrow{u}_2 \\ \delta\overrightarrow{u}_3 \\ \vdots \\ \delta\overrightarrow{u}_N \end{bmatrix} \tag{3.9}$$

and $\mathbf{A}$ is defined as:

$$\mathbf{A} = \begin{bmatrix} J_{bc_1} & J_{bc_2} & 0 & \cdots & \cdots \\ \frac{1}{\Delta x_i} J_2^+ & \frac{1}{\Delta x_i}\left(-J_2^+ + J_2^-\right) + J_{S_2} & -\frac{1}{\Delta x_i} J_2^- & 0 & \cdots \\ 0 & \frac{1}{\Delta x_i} J_3^+ & \frac{1}{\Delta x_i}\left(-J_3^+ + J_3^-\right) + J_{S_3} & -\frac{1}{\Delta x_i} J_3^- & 0 \\ \vdots & 0 & \frac{1}{\Delta x_i} J_4^+ & \ddots & \ddots \\ \vdots & \vdots & 0 & J_{bc_{N-1}} & J_{bc_N} \end{bmatrix} \tag{3.10}$$

The size of the system matrix is $3N$ by $3N$ where N is the total number of grid points. There may be some confusion between the system eigenvalues, which are the eigenvalues of the $\mathbf{A}$ matrix, and the local eigenvalues, which are the characteristics at each lump of the system. A continuous time linear system is stable when all of the eigenvalues of the system matrix have negative real parts. When the spatial derivatives of equation (2.15) are discretized properly, the small perturbation model is stable.

The procedure for the development of the system matrix must be modified when the boundary conditions are taken into consideration. In general, the cowl lip boundary condition is supersonic, represented by J_{bc_1} and J_{bc_2}, and the compressor face boundary condition is subsonic, represented by J_{bc_N} and $J_{bc_{N-1}}$. These boundary conditions are included as modifications to the system matrix at the first and last grid points. They are implemented following the method developed previously and will be discussed at length in the following section where the input matrix term, $\mathbf{B}$, is derived.

3.3 Input Matrix

3.3.1 Downstream Static Pressure

When the flow at the compressor face is subsonic (i.e. $u < c$), there are two numerical boundary conditions and one physical boundary condition. The numerical boundary conditions are associated with the positive characteristics, u and $u+c$, and the physical boundary condition is associated with the negative characteristic, $u - c$. The implementation of the downstream static pressure as a boundary condition input [9] is derived below.

To begin with, take the inverse of (2.17), and then partition the matrix following the procedure from section 2.3.

$$K^{-1} = \begin{bmatrix} \\ (K^{-1})^N \\ \text{----} \\ (K^{-1})^P \end{bmatrix} = \begin{bmatrix} 1 - \frac{1}{2}(\gamma-1)M^2 & \frac{(\gamma-1)u}{c^2} & -\left(\frac{\gamma-1}{c^2}\right) \\ \left[\frac{1}{2}(\gamma-1)u^2 - uc\right]\frac{1}{\rho c} & \frac{c-(\gamma-1)u}{\rho c} & \frac{\gamma-1}{\rho c} \\ \text{----------} & \text{-------} & \text{-----} \\ -\left[\frac{1}{2}(\gamma-1)u^2 + uc\right]\frac{1}{\rho c} & \frac{c+(\gamma-1)u}{\rho c} & -\left(\frac{\gamma-1}{\rho c}\right) \end{bmatrix} \tag{3.11}$$

Here, $\left(K^{-1}\right)^N$ is the first two rows of K^{-1} and $\left(K^{-1}\right)^P$ is the last row of K^{-1}. The physical boundary condition equation is:

$$B_{bc}(\overrightarrow{u}) = p - p_{input} \tag{3.12}$$

where p_{input} is the prescribed boundary condition input, and p is rewritten in terms of the state variables ρ, m, and ε. Equation (3.12) then becomes the following:

$$B_{bc}(\overrightarrow{u}) = (\gamma - 1)\left(\varepsilon - \frac{m^2}{2\rho}\right) - p_{input} \tag{3.13}$$

Taking the partial derivative of $B_{bc}(\overrightarrow{u})$ with respect to $\overrightarrow{u}$ yields,

$$\frac{\partial B_{bc}}{\partial \overrightarrow{u}} = \begin{bmatrix} \frac{\partial p}{\partial \rho} & \frac{\partial p}{\partial m} & \frac{\partial p}{\partial \varepsilon} \end{bmatrix} = \begin{bmatrix} \frac{(\gamma-1)m^2}{2\rho^2} & -\frac{(\gamma-1)m}{\rho} & (\gamma-1) \end{bmatrix} \tag{3.14}$$

Therefore, for the downstream static pressure boundary condition, K_1 (2.32) is defined as:

$$K_1 = \begin{bmatrix} \\ \left(K^{-1}\right)^N \\ \\ \hline \\ \frac{\partial B_{bc}}{\partial \overrightarrow{u}} \\ \\ \end{bmatrix} = \left[\begin{array}{ccc} 1 - \frac{1}{2}(\gamma-1)M^2 & \frac{(\gamma-1)u}{c^2} & -\left(\frac{\gamma-1}{c^2}\right) \\ \left[\frac{1}{2}(\gamma-1)u^2 - uc\right]\frac{1}{\rho c} & \frac{c-(\gamma-1)u}{\rho c} & \frac{\gamma-1}{\rho c} \\ \hline \frac{(\gamma-1)m^2}{2\rho^2} & -\frac{(\gamma-1)m}{\rho} & (\gamma-1) \end{array}\right] \tag{3.15}$$

and K_2 (2.33) is defined as:

$$K_2 = \begin{bmatrix} \\ \left(K^{-1}\right)^N \\ \\ \hline \\ 0 \\ \\ \end{bmatrix} = \left[\begin{array}{ccc} 1 - \frac{1}{2}(\gamma-1)M^2 & \frac{(\gamma-1)u}{c^2} & -\left(\frac{\gamma-1}{c^2}\right) \\ \left[\frac{1}{2}(\gamma-1)u^2 - uc\right]\frac{1}{\rho c} & \frac{c-(\gamma-1)u}{\rho c} & \frac{\gamma-1}{\rho c} \\ \hline 0 & 0 & 0 \end{array}\right] \tag{3.16}$$

From equation (2.34) the compressor face boundary condition may be described as follows.

$$\frac{\partial \overrightarrow{u}_N}{\partial t} + K_1^{-1}K_2J_N\frac{\partial \overrightarrow{u}_N}{\partial x} = K_1^{-1}\begin{bmatrix} \left(K^{-1}\right)^N G(\overrightarrow{u}_N) \\ -B_{bc} \end{bmatrix} \tag{3.17}$$

For this boundary condition to be implemented in the small perturbation model, it must be linearized as shown below.

$$\frac{\partial \delta\overrightarrow{u}_N}{\partial t} + K_1^{-1}K_2J_N\frac{\partial \delta\overrightarrow{u}_N}{\partial x} = K_1^{-1}\begin{bmatrix} \left(K^{-1}\right)^N J_{S_N}\delta\overrightarrow{u}_N \\ -\delta B_{bc} \end{bmatrix} \tag{3.18}$$

δB_{bc} is calculated as:

$$\delta B_{bc} = \frac{\partial B_{bc}}{\partial \overrightarrow{u}}\delta\overrightarrow{u} + \frac{\partial B_{bc}}{\partial p_{input}}\delta p_{input} \tag{3.19}$$

and can be rewritten as:

$$\delta B_{bc} = \begin{bmatrix} \frac{(\gamma-1)m^2}{2\rho^2} & -\frac{(\gamma-1)m}{\rho} & (\gamma-1) \end{bmatrix}\delta\overrightarrow{u} - \delta p_{input} \tag{3.20}$$

Now substituting equation (3.20) into equation (3.18) and replacing $\frac{\partial \delta \overrightarrow{u}_N}{\partial x}$ with equation (2.19) yields:

$$\begin{aligned}\frac{\partial \delta \overrightarrow{u}_N}{\partial t} &= -K_1^{-1} K_2 J_N \left(\frac{\delta \overrightarrow{u}_N - \delta \overrightarrow{u}_{N-1}}{\Delta x_i} \right) \\ &+ K_1^{-1} \begin{bmatrix} & \left(K^{-1}\right)^N J_{S_N} & \\ -\frac{(\gamma-1)m^2}{2\rho^2} & \frac{(\gamma-1)m}{\rho} & -(\gamma-1) \end{bmatrix} \delta \overrightarrow{u}_N \\ &+ K_1^{-1} \begin{bmatrix} 0 \\ 0 \\ 1 \end{bmatrix} \delta p_{input}\end{aligned} \tag{3.21}$$

Equation (3.22) is used to modify the system matrix, (3.10), at the last grid point.

$$\frac{\partial \delta \overrightarrow{u}_N}{\partial t} = J_{bc_N} \delta \overrightarrow{u}_N + J_{bc_{N-1}} \delta \overrightarrow{u}_{N-1} + K_1^{-1} \begin{bmatrix} 0 \\ 0 \\ 1 \end{bmatrix} \delta p_{input} \tag{3.22}$$

The terms for J_{bc_N}, $J_{bc_{N-1}}$, and K_1^{-1} are defined as follows:

$$\begin{aligned} J_{bc_N} &= \frac{-K_1^{-1} K_2 J_N}{\Delta x_i} + K_1^{-1} \begin{bmatrix} & \left(K^{-1}\right)^N J_{S_N} & \\ -\frac{(\gamma-1)m^2}{2\rho^2} & \frac{(\gamma-1)m}{\rho} & -(\gamma-1) \end{bmatrix} \\ J_{bc_{N-1}} &= \frac{K_1^{-1} K_2 J_N}{\Delta x_i} \\ K_1^{-1} &= \begin{bmatrix} & \left(K^{-1}\right)^N & \\ \frac{\partial p}{\partial \rho} & \frac{\partial p}{\partial m} & \frac{\partial p}{\partial \varepsilon} \end{bmatrix}^{-1} \end{aligned} \tag{3.23}$$

The terms for the input matrix, $\mathbf{B}$, are obtained from the coefficient on δp_{input} from equation (3.22).

3.3.2 Downstream Mach Number

As was the case for the downstream pressure, the input matrix for the downstream Mach number follows directly from the implementation of the compressor face boundary condition. The physical boundary condition equation is:

$$B_{bc}(\overrightarrow{u}) = M - M_{input} \tag{3.24}$$

where M is defined as:

$$M = \frac{u}{c} \tag{3.25}$$

Rewrite M in terms of ρ, m, and ε,

$$M = \frac{m}{\sqrt{\gamma\rho(\gamma-1)\left(\varepsilon - \frac{m^2}{2\rho}\right)}} = \frac{\sqrt{2}m\,\mathrm{sgn}(\rho)}{\sqrt{\gamma\left(2\varepsilon\rho(\gamma-1) - \gamma m^2 + m^2\right)}} \tag{3.26}$$

and follow the same procedure that was used for the downstream pressure input. Equation (3.27) is used to modify the system matrix at the last grid point.

$$\frac{\partial \delta \vec{u}_N}{\partial t} = J_{bc_N} \delta \vec{u}_N + J_{bc_{N-1}} \delta \vec{u}_{N-1} + K_1^{-1} \begin{bmatrix} 0 \\ 0 \\ 1 \end{bmatrix} \delta M_{input} \tag{3.27}$$

The terms for J_{bc_N} and $J_{bc_{N-1}}$, and K_1^{-1} are defined as follows:

$$J_{bc_N} = \frac{-K_1^{-1} K_2 J_N}{\Delta x_i} + K_1^{-1} \begin{bmatrix} & \left(K^{-1}\right)^N J_{S_N} & \\ -\frac{\partial M}{\partial \rho} & -\frac{\partial M}{\partial m} & -\frac{\partial M}{\partial \varepsilon} \end{bmatrix}$$

$$J_{bc_{N-1}} = \frac{K_1^{-1} K_2 J_N}{\Delta x_i} \tag{3.28}$$

$$K_1^{-1} = \begin{bmatrix} & \left(K^{-1}\right)^N & \\ \frac{\partial M}{\partial \rho} & \frac{\partial M}{\partial m} & \frac{\partial M}{\partial \varepsilon} \end{bmatrix}^{-1}$$

and $\frac{\partial M}{\partial \rho}$, $\frac{\partial M}{\partial m}$, and $\frac{\partial M}{\partial \varepsilon}$ are shown below.

$$\begin{aligned} \frac{\partial M}{\partial \rho} &= \frac{\sqrt{2}\varepsilon m \sqrt{\gamma\left(2\varepsilon\rho\left(\gamma-1\right)-\gamma m^2+m^2\right)}\,\mathrm{sgn}\left(\rho\right)}{\gamma\left(2\varepsilon\rho-m^2\right)^2\left(1-\gamma\right)} \\ \frac{\partial M}{\partial m} &= \frac{2\sqrt{2}\varepsilon\left|\rho\right|}{\left(2\varepsilon\rho-m^2\right)\sqrt{\gamma\left(2\varepsilon\rho\left(\gamma-1\right)-\gamma m^2+m^2\right)}} \\ \frac{\partial M}{\partial \varepsilon} &= \frac{\sqrt{2} m \sqrt{\gamma\left(2\varepsilon\rho\left(\gamma-1\right)-\gamma m^2+m^2\right)}\left|\rho\right|}{\gamma\left(2\varepsilon\rho-m^2\right)^2\left(1-\gamma\right)} \end{aligned} \tag{3.29}$$

The terms for the input matrix are obtained from the coefficient on δM_{input} from equation (3.27).

3.3.3 Downstream Corrected Massflow

Again, the input matrix for the downstream corrected massflow follows directly from the implementation of the compressor face boundary condition. The physical boundary condition equation is:

$$B_{bc}(\vec{u}) = \dot{m}_c - \dot{m}_{c_{input}} \tag{3.30}$$

where $\dot{m}_c$ is defined as:

$$\dot{m}_c = mA \frac{\sqrt{T_t}}{p_t} \frac{p_{sl}}{\sqrt{T_{sl}}} \tag{3.31}$$

Rewrite $\dot{m}_c$ in terms of ρ, m, and ε,

$$\dot{m}_c = \sqrt{2} A \gamma m p_{sl}\,\mathrm{sgn}\left(\rho\right) \frac{\sqrt{\frac{2\varepsilon\gamma\rho\left(\gamma-1\right)-\gamma^2 m^2+2\gamma m^2-m^2}{\gamma R T_{sl}}} \left(\frac{2\varepsilon\gamma\rho+m^2\left(1-\gamma\right)}{\gamma\left(2\varepsilon\rho-m^2\right)}\right)^{\frac{1}{1-\gamma}}}{\left(2\varepsilon\gamma\rho+m^2\left(1-\gamma\right)\right)\left(\gamma-1\right)} \tag{3.32}$$

and follow the same procedure that was used for the downstream pressure input. Equation (3.33) is used to modify the system matrix at the last grid point.

$$\frac{\partial \delta \vec{u}_N}{\partial t} = J_{bc_N} \delta \vec{u}_N + J_{bc_{N-1}} \delta \vec{u}_{N-1} + K_1^{-1} \begin{bmatrix} 0 \\ 0 \\ 1 \end{bmatrix} \delta \dot{m}_{cinput} \tag{3.33}$$

The terms for J_{bc_N}, $J_{bc_{N-1}}$, and K_1^{-1} are defined as follows:

$$J_{bc_N} = \frac{-K_1^{-1} K_2 J_N}{\Delta x_i} + K_1^{-1} \begin{bmatrix} & \left(K^{-1}\right)^N J_{S_N} & \\ -\frac{\partial \dot{m}_c}{\partial \rho} & -\frac{\partial \dot{m}_c}{\partial m} & -\frac{\partial \dot{m}_c}{\partial \varepsilon} \end{bmatrix}$$

$$J_{bc_{N-1}} = \frac{K_1^{-1} K_2 J_N}{\Delta x_i} \tag{3.34}$$

$$K_1^{-1} = \begin{bmatrix} & \left(K^{-1}\right)^N & \\ \frac{\partial \dot{m}_c}{\partial \rho} & \frac{\partial \dot{m}_c}{\partial m} & \frac{\partial \dot{m}_c}{\partial \varepsilon} \end{bmatrix}^{-1}$$

and $\frac{\partial \dot{m}_c}{\partial \rho}$, $\frac{\partial \dot{m}_c}{\partial m}$, and $\frac{\partial \dot{m}_c}{\partial \varepsilon}$ are shown below.

$$\begin{aligned}
\frac{\partial \dot{m}_c}{\partial \rho} &= \frac{\sqrt{2} A \gamma \varepsilon m p_{sl} \operatorname{sgn}(\rho) \operatorname{var}_1 \operatorname{var}_2 \operatorname{var}_3}{\left(2\varepsilon\gamma\rho + m^2(1-\gamma)\right)^2 \left(m^2 - 2\varepsilon\rho\right)(\gamma-1)^2} \\
\frac{\partial \dot{m}_c}{\partial m} &= \frac{2\sqrt{2} A \varepsilon \gamma p_{sl} |\rho| \operatorname{var}_1 \operatorname{var}_2 \operatorname{var}_3}{\left(2\varepsilon\gamma\rho + m^2(1-\gamma)\right)^2 \left(2\varepsilon\rho - m^2\right)(\gamma-1)^2} \\
\frac{\partial \dot{m}_c}{\partial \varepsilon} &= \frac{\sqrt{2} A \gamma m p_{sl} |\rho| \operatorname{var}_1 \operatorname{var}_2 \operatorname{var}_3}{\left(2\varepsilon\gamma\rho + m^2(1-\gamma)\right)^2 \left(m^2 - 2\varepsilon\rho\right)(\gamma-1)^2} \\
\operatorname{var}_1 &= 2\varepsilon\gamma\rho(\gamma-1) - m^2\left(\gamma^2 - \gamma + 2\right) \\
\operatorname{var}_2 &= \sqrt{\frac{2\varepsilon\gamma\rho(\gamma-1) - \gamma^2 m^2 + 2\gamma m^2 - m^2}{\gamma R T_{sl}}} \\
\operatorname{var}_3 &= \left(\frac{2\varepsilon\gamma\rho + m^2(1-\gamma)}{\gamma\left(2\varepsilon\rho - m^2\right)}\right)^{\frac{1}{1-\gamma}}
\end{aligned} \tag{3.35}$$

The terms for the input matrix are obtained from the coefficient on $\delta \dot{m}_{cinput}$ from equation (3.33).

3.3.4 Upstream Mach Number

Following the procedure developed for the downstream boundary condition input, the upstream Mach number input is implemented in the following manner. When the flow at the cowl lip is supersonic, there are

zero numerical boundary conditions and three physical boundary conditions. The three physical boundary conditions are associated with the positive characteristics u, $u+c$, and $u-c$. Therefore, $\left(K^{-1}\right)^N = 0$ and $\left(K^{-1}\right)^P = K^{-1}$. The physical boundary condition definition is:

$$B_{bc}(\overrightarrow{u}) = \begin{bmatrix} \rho \\ M - M_{input} \\ \varepsilon \end{bmatrix} \tag{3.36}$$

The input is associated with the second characteristic because the third characteristic is needed if the boundary condition were subsonic, and the first characteristic usually results in a nonsingularity for equation (2.31). M_{input} is the prescribed boundary condition input, and M is replaced in terms of the state variables ρ, m, and ε. Take the partial derivative of $B_{bc}(\overrightarrow{u})$ with respect to $\overrightarrow{u}$.

$$\frac{\partial B_{bc}}{\partial \overrightarrow{u}} = \begin{bmatrix} 1 & 0 & 0 \\ \frac{\partial M}{\partial \rho} & \frac{\partial M}{\partial m} & \frac{\partial M}{\partial \varepsilon} \\ 0 & 0 & 1 \end{bmatrix} \tag{3.37}$$

Using the previous definitions for K_1 and K_2, they become $K_1 = \frac{\partial B_{bc}}{\partial \overrightarrow{u}}$, and $K_2 = 0$. The cowl lip boundary condition is represented by the following equation.

$$\frac{\partial \overrightarrow{u}_1}{\partial t} + K_1^{-1} K_2 J_1 \frac{\partial \overrightarrow{u}_1}{\partial x} = K_1^{-1} \begin{bmatrix} \left(K^{-1}\right)^N G(\overrightarrow{u}_1) \\ -B_{bc} \end{bmatrix} \tag{3.38}$$

To be implemented in the small perturbation model, equation (3.38) must be linearized as shown in the next equation.

$$\frac{\partial \delta\overrightarrow{u}_1}{\partial t} + K_1^{-1} K_2 J_1 \frac{\partial \delta\overrightarrow{u}_1}{\partial x} = K_1^{-1} \begin{bmatrix} \left(K^{-1}\right)^N J_{S_1} \delta\overrightarrow{u}_1 \\ -\delta B_{bc} \end{bmatrix} \tag{3.39}$$

δB_{bc} is calculated as:

$$\delta B_{bc} = \frac{\partial B_{bc}}{\partial \overrightarrow{u}} \delta\overrightarrow{u} + \frac{\partial B_{bc}}{\partial M_{input}} \delta M_{input} \tag{3.40}$$

Now, δB_{bc} can be rewritten as:

$$\delta B_{bc} = \begin{bmatrix} 1 & 0 & 0 \\ \frac{\partial M}{\partial \rho} & \frac{\partial M}{\partial m} & \frac{\partial M}{\partial \varepsilon} \\ 0 & 0 & 1 \end{bmatrix} \delta\overrightarrow{u} - \delta M_{input} \tag{3.41}$$

Then substitute equation (3.41) into equation (3.39), and replace $\frac{\partial \delta\overrightarrow{u}_1}{\partial x}$ with equation (2.20).

$$\begin{aligned} \frac{\partial \delta\overrightarrow{u}_1}{\partial t} \;=\; & -K_1^{-1} K_2 J_1 \left(\frac{\delta\overrightarrow{u}_2 - \delta\overrightarrow{u}_1}{\Delta x_i} \right) \\ & + K_1^{-1} \begin{bmatrix} \left(K^{-1}\right)^N J_{S_1} \\ -\frac{\partial B_{bc}}{\partial \overrightarrow{u}} \end{bmatrix} \delta\overrightarrow{u}_1 \\ & + K_1^{-1} \begin{bmatrix} 0 \\ 1 \\ 0 \end{bmatrix} \delta M_{input} \end{aligned} \tag{3.42}$$

Equation (3.43) is used to modify the system matrix at the first grid point.

$$\frac{\partial \delta \vec{u}_N}{\partial t} = J_{bc_1} \delta \vec{u}_1 + J_{bc_2} \delta \vec{u}_2 + K_1^{-1} \begin{bmatrix} 0 \\ 1 \\ 0 \end{bmatrix} \delta M_{input} \tag{3.43}$$

The terms for J_{bc_1}, J_{bc_2}, and K_1^{-1} are defined as follows:

$$J_{bc_1} = -K_1^{-1} \begin{bmatrix} 1 & 0 & 0 \\ \frac{\partial M}{\partial \rho} & \frac{\partial M}{\partial m} & \frac{\partial M}{\partial \varepsilon} \\ 0 & 0 & 1 \end{bmatrix}$$

$$J_{bc_2} = 0 \tag{3.44}$$

$$K_1^{-1} = \begin{bmatrix} 1 & 0 & 0 \\ \frac{\partial M}{\partial \rho} & \frac{\partial M}{\partial m} & \frac{\partial M}{\partial \varepsilon} \\ 0 & 0 & 1 \end{bmatrix}^{-1}$$

The terms for the input matrix are obtained from the coefficient on δM_{input} from equation (3.43).

3.3.5 Upstream Static Temperature

Again, the input matrix for the upstream static temperature input follows directly from the implementation of the cowl lip boundary condition. The physical boundary condition equation is:

$$B_{bc}(\vec{u}) = T - T_{input} \tag{3.45}$$

where T is defined as:

$$T = \frac{p}{\rho R} \tag{3.46}$$

Rewrite T in terms of ρ, m, and ε,

$$T = \frac{1}{\rho R}(\gamma - 1)\left(\varepsilon - \frac{m^2}{2\rho}\right) \tag{3.47}$$

and follow the same procedure that was used for the upstream Mach number input. Equation (3.48) is used to modify the system matrix at the first grid point.

$$\frac{\partial \delta \vec{u}_N}{\partial t} = J_{bc_1} \delta \vec{u}_1 + J_{bc_2} \delta \vec{u}_2 + K_1^{-1} \begin{bmatrix} 0 \\ 1 \\ 0 \end{bmatrix} \delta T_{input} \tag{3.48}$$

The terms for J_{bc_1}, J_{bc_2}, and K_1^{-1} are defined as follows:

$$J_{bc_1} = -K_1^{-1} \begin{bmatrix} 1 & 0 & 0 \\ \frac{\partial T}{\partial \rho} & \frac{\partial T}{\partial m} & \frac{\partial T}{\partial \varepsilon} \\ 0 & 0 & 1 \end{bmatrix}$$

$$J_{bc_2} = 0 \tag{3.49}$$

$$K_1^{-1} = \begin{bmatrix} 1 & 0 & 0 \\ \frac{\partial T}{\partial \rho} & \frac{\partial T}{\partial m} & \frac{\partial T}{\partial \varepsilon} \\ 0 & 0 & 1 \end{bmatrix}^{-1}$$

and $\frac{\partial T}{\partial \rho}$, $\frac{\partial T}{\partial m}$, and $\frac{\partial T}{\partial \varepsilon}$ are shown below.

$$\begin{aligned} \frac{\partial T}{\partial \rho} &= \frac{m^2(\gamma^2 - 2\gamma + 1) - \varepsilon\gamma\rho(\gamma - 1)}{\gamma R \rho^3} \\ \frac{\partial T}{\partial m} &= -\frac{m(\gamma^2 - 2\gamma + 1)}{\gamma R \rho^2} \\ \frac{\partial T}{\partial \varepsilon} &= \frac{(\gamma - 1)}{R\rho} \end{aligned} \tag{3.50}$$

The terms for the input matrix are obtained from the coefficient on δT_{input} from equation (3.48).

3.3.6 Downstream Bypass Massflow

Implementation of the downstream bypass massflow input requires that the source terms, M_S, F_S, and Q_S, be added to the right hand side of the governing equations [8] as shown in equation (3.51).

$$\frac{\partial \vec{u}}{\partial t} + \frac{\partial F(\vec{u})}{\partial x} = G(\vec{u}) + \begin{bmatrix} M_S \\ F_S \\ Q_S \end{bmatrix} \tag{3.51}$$

The source terms are defined by (3.52) through (3.54).

Mass Transfer Continuity Term:

$$M_S = \frac{1}{A_i}\frac{d\,\dot{m}_i}{dx} \tag{3.52}$$

Mass Transfer Momentum Term:

$$F_S = \frac{u_i}{A_i}\frac{d\,\dot{m}_i}{dx} \tag{3.53}$$

Mass Transfer Energy Term:

$$Q_S = \frac{1}{A_i}\left(\frac{\varepsilon_i + p_i}{\rho_i}\right)\frac{d\,\dot{m}_i}{dx} \tag{3.54}$$

Here, $\frac{d\,\dot{m}_i}{dx}$ is the massflow transferred across the wall of the ith control volume divided by the control volume length; in steady state, this is equal to the massflow in the inlet minus the massflow at the cowl lip.

$$d\,\dot{m} = \dot{m}_i - \dot{m}_{cowl\,lip} \tag{3.55}$$

But in order to have the bypass massflow, $\dot{m}_{bypass}$, as an input to the model, equation (3.55) needs to be rewritten with this term. Since the massflow is a conserved quantity, it can be expressed as the following:

$$\dot{m}_{cowl\,lip} = \dot{m}_{bypass} + \dot{m}_{compressor\,face} \tag{3.56}$$

with this substitution for $\dot{m}_{cowl\,lip}$ equation (3.55) becomes:

$$d\,\dot{m}_i = \dot{m}_i - \left(\dot{m}_{bypass} + \dot{m}_{compressor\,face}\right) \tag{3.57}$$

Now the source terms for the bypass massflow can be defined as:

$$\begin{aligned} M_S &= \frac{1}{A_i}\left(\frac{\dot{m}_i - \dot{m}_{bypass} - \dot{m}_{compressor\,face}}{\Delta x_i}\right) \\ F_S &= \frac{u_i}{A_i}\left(\frac{\dot{m}_i - \dot{m}_{bypass} - \dot{m}_{compressor\,face}}{\Delta x_i}\right) \\ Q_S &= \frac{(\varepsilon_i + p_i)}{\rho_i A_i}\left(\frac{\dot{m}_i - \dot{m}_{bypass} - \dot{m}_{compressor\,face}}{\Delta x_i}\right) \end{aligned} \tag{3.58}$$

and linearized with respect to $\dot{m}_{bypass}$.

$$\mathbf{B}\;\delta\,\dot{m}_{bypass} = \begin{bmatrix} \delta M_S \\ \delta F_S \\ \delta Q_S \end{bmatrix} \delta\,\dot{m}_{bypass} = \begin{bmatrix} \frac{-1}{A_i \Delta x_i} \\ \frac{-u_i}{A_i \Delta x_i} \\ \frac{-(\varepsilon_i + p_i)}{\rho_i A_i \Delta x_i} \end{bmatrix} \delta\,\dot{m}_{bypass} \tag{3.59}$$

The terms for the input matrix are obtained from the coefficients on $\delta\,\dot{m}_{bypass}$.

3.3.7 Throat Bleed Massflow

The throat bleed massflow input is implemented using the same method as for the downstream bypass massflow input. In this case, the bleed massflow is expressed as:

$$\dot{m}_{cowl\,lip} = \dot{m}_{bleed} + \dot{m}_{compressor\,face} \tag{3.60}$$

The source terms for the bleed massflow are defined as:

$$\begin{aligned} M_S &= \frac{1}{A_i}\left(\frac{\dot{m}_i - \dot{m}_{bleed} - \dot{m}_{compressor\,face}}{\Delta x_i}\right) \\ F_S &= \frac{u_i}{A_i}\left(\frac{\dot{m}_i - \dot{m}_{bleed} - \dot{m}_{compressor\,face}}{\Delta x_i}\right) \\ Q_S &= \frac{(\varepsilon_i + p_i)}{\rho_i A_i}\left(\frac{\dot{m}_i - \dot{m}_{bleed} - \dot{m}_{compressor\,face}}{\Delta x_i}\right) \end{aligned} \tag{3.61}$$

and linearized with respect to $\dot{m}_{bleed}$.

$$\mathbf{B}\;\delta\,\dot{m}_{bleed} = \begin{bmatrix} \delta M_S \\ \delta F_S \\ \delta Q_S \end{bmatrix} \delta\,\dot{m}_{bleed} = \begin{bmatrix} \frac{-1}{A_i \Delta x_i} \\ \frac{-u_i}{A_i \Delta x_i} \\ \frac{-(\varepsilon_i + p_i)}{\rho_i A_i \Delta x_i} \end{bmatrix} \delta\,\dot{m}_{bleed} \tag{3.62}$$

The terms for the input matrix are obtained from the coefficients on $\delta\,\dot{m}_{bleed}$.

3.4 Output Matrix

3.4.1 Static Pressure

The components of the output matrix, **C**, for the static pressure response are obtained by linearizing the static pressure equation:

$$\begin{aligned} p &= (\gamma-1)\left(\varepsilon-\frac{m^2}{2\rho}\right) \\ \delta p &= \frac{\partial p}{\partial \rho}\delta\rho+\frac{\partial p}{\partial m}\delta m+\frac{\partial p}{\partial \varepsilon}\delta\varepsilon \\ \delta p &= \frac{1}{2}(\gamma-1)\left(\frac{m}{\rho}\right)^2\delta\rho-(\gamma-1)\left(\frac{m}{\rho^2}\right)\delta m+(\gamma-1)\,\delta\varepsilon \end{aligned} \tag{3.63}$$

Each coefficient of the small perturbation terms is an entry in the output matrix.

3.4.2 Total Pressure

The output equation for the total pressure is determined in the same manner as for the static pressure. The components of the output matrix for the total pressure response are obtained from the linearization of the total pressure equation:

$$p_t = p\left(1+\frac{\gamma-1}{2}M^2\right)^{\frac{\gamma}{\gamma-1}} \tag{3.64}$$

The pressure and Mach number terms are replaced with expressions in terms of ρ, m, and ε,

$$p_t = \frac{(\gamma-1)\left(2\varepsilon\gamma\rho+m^2(1-\gamma)\right)\left(\frac{2\varepsilon\gamma\rho+m^2(1-\gamma)}{\gamma(2\varepsilon\rho-m^2)}\right)^{\frac{1}{\gamma-1}}}{2\gamma\rho} \tag{3.65}$$

Then the partial derivative with respect to the state variables is performed as shown below.

$$\delta p_t = \frac{\partial p_t}{\partial \rho}\delta\rho+\frac{\partial p_t}{\partial m}\delta m+\frac{\partial p_t}{\partial \varepsilon}\delta\varepsilon \tag{3.66}$$

Each one of the coefficients on the small perturbation terms in the above equation is an entry in the output matrix for the total pressure.

$$\begin{aligned} \frac{\partial p_t}{\partial \rho} &= \frac{m^2\left(2\varepsilon\gamma\rho(\gamma-2)-m^2(\gamma-1)^2\right)\left(\frac{2\varepsilon\rho+m^2(1-\gamma)}{\gamma(2\varepsilon\rho-m^2)}\right)^{\frac{1}{\gamma-1}}}{2\gamma\rho^2(2\varepsilon\rho-m^2)} \\ \frac{\partial p_t}{\partial m} &= \left(\frac{m^3}{\gamma(2\varepsilon\rho-m^2)}+\frac{m(2-\gamma)}{\rho}\right)\left(\frac{2\varepsilon\rho+m^2(1-\gamma)}{\gamma(2\varepsilon\rho-m^2)}\right)^{\frac{1}{\gamma-1}} \\ \frac{\partial p_t}{\partial \varepsilon} &= -\left(\frac{m^2}{\gamma(2\varepsilon\rho-m^2)}-\gamma+1\right)\left(\frac{2\varepsilon\rho+m^2(1-\gamma)}{\gamma(2\varepsilon\rho-m^2)}\right)^{\frac{1}{\gamma-1}} \end{aligned} \tag{3.67}$$

3.4.3 Mach Number

Likewise, the output equation for the Mach number is determined in the same manner. The components of the output matrix for the Mach number response are obtained from the linearization of the Mach number equation,

$$M = \frac{u}{c} \tag{3.68}$$

The velocity and speed of sound terms are replaced with expressions in terms of ρ, m, and ε (as shown in section 3.3.2). Again, the partial derivative with respect to the state variables is performed,

$$\delta M = \frac{\partial M}{\partial \rho}\delta\rho + \frac{\partial M}{\partial m}\delta m + \frac{\partial M}{\partial \varepsilon}\delta\varepsilon \tag{3.69}$$

and each coefficient on the small perturbation terms is an entry in the output matrix for the Mach number.

$$\begin{aligned}
\frac{\partial M}{\partial \rho} &= \frac{\sqrt{2}\varepsilon m\sqrt{\gamma\left(2\varepsilon\rho\left(\gamma-1\right)-\gamma m^2+m^2\right)}\,\mathrm{sgn}\left(\rho\right)}{\gamma\left(2\varepsilon\rho-m^2\right)^2\left(1-\gamma\right)} \\
\frac{\partial M}{\partial m} &= \frac{2\sqrt{2}\varepsilon\left|\rho\right|}{\left(2\varepsilon\rho-m^2\right)\sqrt{\gamma\left(2\varepsilon\rho\left(\gamma-1\right)-\gamma m^2+m^2\right)}} \\
\frac{\partial M}{\partial \varepsilon} &= \frac{\sqrt{2}m\sqrt{\gamma\left(2\varepsilon\rho\left(\gamma-1\right)-\gamma m^2+m^2\right)}\left|\rho\right|}{\gamma\left(2\varepsilon\rho-m^2\right)^2\left(1-\gamma\right)}
\end{aligned} \tag{3.70}$$

4 Model Reduction

The models developed from the linearized split flux method have the same number of states as the CFD code on which they are based. These models are usually too large to be used effectively in the design of a control system; therefore, model reduction is necessary so that the linear model can be transformed into one that is of manageable size. In addition, a reduced order model (ROM) is needed when a transfer function of the system is desired because calculation of the transfer function from the full order model (FOM) becomes a numerically ill-conditioned problem if there are a large number of state equations. In general, the linear reduced order model is expected to perform like the linear full order model. There are many different methods that can be used for model reduction; those considered here take advantage of the state space format of the linear model.

One of the most common model reduction methods is singular perturbation [11]. This method requires a linear model that can be partitioned into slow and fast subsystems so that a reduced order model can be obtained by neglecting the fast subsystem. The ability to partition the system into subsystems indicates that the model possesses a two-time scale property; that is, there is a large gap in the spread of the eigenvalues of the linear model. There is little contribution to the dynamics of the system from the fast eigenvalues; therefore they can be discarded and reduced order model obtained. But as was shown in [12] this method does not provide the smallest reduced order model that can be achieved.

Another popular method is balancing [13] [14] [15]. This method requires a linear model that can be partitioned into a strongly controllable/observable subsystem and a least controllable/observable subsystem. A reduced order model can then be obtained by discarding the least controllable/observable subsystem. However, the ability to partition the system into these subsystems indicates that the model is minimal; that is, it is both controllable and observable. In general, linear models developed from the linearized CFD

method are not minimal. Therefore this method does not work well because of the many uncontrollable and unobservable states in the linear model.

Two model reduction methods that can be successfully applied to the linear model are the Schur and square root methods [16]. Both of these methods take into account the controllability and observability of the linear system, but they do not depend on the linear model being minimal. The square root method is preferred over the Schur method because it is computationally less expensive. In addition, smaller reduced order models can be extracted from the original reduced order model without any more computations. The same is not true for the Schur method. The square root method is described in the next section and will be applied to the linear models developed later in the paper.

4.1 Square Root Model Reduction

The square root method of model reduction detailed in [16] is summarized here for the readers convenience. This model reduction method reduces the full order model by a balancing transformation that requires only the first k (size of reduced order model) columns of the balancing transformation matrix. The reduced order model $(\mathbf{A}_k, \mathbf{B}_k, \mathbf{C}_k, \mathbf{D}_k)$ for the state space system $(\mathbf{A}, \mathbf{B}, \mathbf{C}, \mathbf{D})$ is calculated from:

$$\begin{aligned} \mathbf{A}_k &= S_{L,big}^T \mathbf{A} S_{R,big} \\ \mathbf{B}_k &= S_{L,big}^T \mathbf{B} \\ \mathbf{C}_k &= \mathbf{C} S_{R,big} \\ \mathbf{D}_k &= \mathbf{D} \end{aligned} \tag{4.1}$$

Determination of the transformation matrices $S_{L,big}^T$ and $S_{R,big}$ is shown below.

The controllability and observability Grammians, P and Q, are calculated from the following Liapunov equations.

$$\begin{aligned} \mathbf{A}P + P\mathbf{A}^T &= -\mathbf{B}\mathbf{B}^T \\ \mathbf{A}^T Q + Q\mathbf{A} &= -\mathbf{C}^T\mathbf{C} \end{aligned} \tag{4.2}$$

Once the Liapunov equations are solved for the Grammians, the square roots of P and Q are calculated.

$$\begin{aligned} L_c L_c^T &= P \\ L_o L_o^T &= Q \end{aligned} \tag{4.3}$$

A singular value decomposition of $L_o^T L_c$ produces the matrices needed to compute $S_{L,big}^T$ and $S_{R,big}$.

$$U \sum_1 V^T = L_o^T L_c \tag{4.4}$$

$\sum_1$ is defined as:

$$\sum_1 = diag(\sigma_1, \sigma_2, \cdots, \sigma_m) \tag{4.5}$$

where m is the number of nonzero Hankel singular values represented by σ. The σ are defined as the square roots of the eigenvalues of the PQ matrix.

$$\sigma = (\lambda(PQ))^{\frac{1}{2}} \tag{4.6}$$

From $\sum_1$, $\sum_{bal}$ is defined as $\sum_{bal} = diag(\sigma_1, \sigma_2, \cdots, \sigma_k)$. Note that the σ are in descending order according to their magnitude. Now $S_{L,big}$ and $S_{R,big}$ can be calculated from the following equations,

$$\begin{aligned} S_{L,big} &= L_o U \begin{bmatrix} \sum_{bal}^{-\frac{1}{2}} \\ 0 \end{bmatrix} \\ S_{R,big} &= L_c V \begin{bmatrix} \sum_{bal}^{-\frac{1}{2}} \\ 0 \end{bmatrix} \end{aligned} \tag{4.7}$$

and the reduced order model can be determined using equation (4.1). Determination of the size of the reduced order model and the error associated with the model reduction process are described in the next section.

5 Uncertainty

The major source of error incurred in developing linear control models lies in the linearization process. As long as all the expected perturbations from steady-state are "small", the error bounds will be small. Small, here, depends upon which variables are being considered and how sensitive the system dynamics are to steady-state changes. Clearly this must be determined by trial and error for each system considered. Normalizing the data allows all the variables to be weighted similarly. Many approaches could be considered for determining error bounds. The one described below uses infinity norm bounds and is probably the most useful for the control system designer; in addition, it is also a convenient form for the numerical experiments considered. It should be noted that this error bound holds exactly only for linear systems; as such, it only serves as an approximation of the true bound. Its accuracy will certainly be degraded for larger perturbations.

There is a certain amount of error associated with the linear models developed using the linearized split flux method; in particular, there is error due to the linearization process and the model reduction process. These errors can be characterized as modeling uncertainties which are represented by error bounds and are derived below.

5.1 Linearization Error

The modeling error due to the linearization process is based on the fact that the infinity norm of the transfer function error is less than or equal to the one norm of the unit impulse response error (B. Veillette, University of Akron, Akron, OH., private communication).

$$\|\mathbf{G}(j\omega)_{true} - \mathbf{G}(j\omega)\|_\infty \leqslant \|\mathbf{g}_{true}(t) - \mathbf{g}(t)\|_1 \tag{5.1}$$

$\mathbf{G}(j\omega)_{true}$ represents the transfer function of an exact linear model, if it were available, and $\mathbf{G}(j\omega)$ represents the transfer function from the split flux linearization process. The infinity norm of the transfer function error is defined as:

$$\|\mathbf{G}(j\omega)_{true} - \mathbf{G}(j\omega)\|_\infty = \sigma_{\max}\{\mathbf{G}(j\omega)_{true} - \mathbf{G}(j\omega)\} \tag{5.2}$$

and the one norm of the impulse response error is defined as:

$$\|\mathbf{g}_{true}(t) - \mathbf{g}(t)\|_1 = \int_0^\infty |\mathbf{g}_{true}(t) - \mathbf{g}(t)|\, dt \tag{5.3}$$

$\int_0^\infty |\mathbf{g}_{true}(t) - \mathbf{g}(t)|\, dt$ can be approximated by:

$$\int_0^\infty |\mathbf{g}_{true}(t) - \mathbf{g}(t)|\, dt \simeq \sum_{n=0}^{\mathbf{N}} |\mathbf{g}^n_{true} - \mathbf{g}^n|\, \Delta T \tag{5.4}$$

Therefore, the error bound on the infinity norm of the transfer function can be represented by the following:

$$\|\mathbf{G}(j\omega)_{true} - \mathbf{G}(j\omega)\|_\infty \lesssim \sum_{n=0}^{\mathbf{N}} |\mathbf{g}^n_{true} - \mathbf{g}^n|\, \Delta T \tag{5.5}$$

The notation can be simplified by expressing $\mathbf{G}(j\omega)_{true} - \mathbf{G}(j\omega)$ as $\mathbf{E}(j\omega)$ and $\mathbf{g}^n_{true} - \mathbf{g}^n$ as $\mathbf{e}^n$. Therefore, the linearization error bound is represented as:

$$\|\mathbf{E}(j\omega)\|_\infty \lesssim \sum_{n=0}^{\mathbf{N}} |\mathbf{e}^n|\, \Delta T \tag{5.6}$$

For multi-input/multi-output systems (MIMO), the transfer functions and impulse responses are represented in matrix form, and the linearization error bound can be determined from the following:

$$\|\mathbf{E}(j\omega)\|_\infty \lesssim \sigma_{\max}\left\{\begin{bmatrix} \|\mathbf{e}_{11}(t)\|_1 & \|\mathbf{e}_{12}(t)\|_1 & \cdots & \|\mathbf{e}_{1p}(t)\|_1 \\ \|\mathbf{e}_{21}(t)\|_1 & \|\mathbf{e}_{22}(t)\|_1 & \cdots & \|\mathbf{e}_{2p}(t)\|_1 \\ \vdots & \vdots & \ddots & \vdots \\ \|\mathbf{e}_{r1}(t)\|_1 & \|\mathbf{e}_{r2}(t)\|_1 & \cdots & \|\mathbf{e}_{rp}(t)\|_1 \end{bmatrix}\right\} \tag{5.7}$$

The maximum singular value of a matrix is defined as:

$$\sigma_{\max} = \left(\lambda_{\max}\left(matrix^T matrix\right)\right)^{\frac{1}{2}} \tag{5.8}$$

For a MIMO system with p number of inputs and r number of outputs, the transfer function error matrix is written as:

$$\mathbf{E}(j\omega) = \begin{bmatrix} \mathbf{E}_{11}(j\omega) & \mathbf{E}_{12}(j\omega) & \cdots & \mathbf{E}_{1p}(j\omega) \\ \mathbf{E}_{21}(j\omega) & \mathbf{E}_{22}(j\omega) & \cdots & \mathbf{E}_{2p}(j\omega) \\ \vdots & \vdots & \ddots & \vdots \\ \mathbf{E}_{r1}(j\omega) & \mathbf{E}_{r2}(j\omega) & \cdots & \mathbf{E}_{rp}(j\omega) \end{bmatrix} \tag{5.9}$$

and the impulse error matrix is written as:

$$\mathbf{e}(t) = \begin{bmatrix} \mathbf{e}_{11}(t) & \mathbf{e}_{12}(t) & \cdots & \mathbf{e}_{1p}(t) \\ \mathbf{e}_{21}(t) & \mathbf{e}_{22}(t) & \cdots & \mathbf{e}_{2p}(t) \\ \vdots & \vdots & \ddots & \vdots \\ \mathbf{e}_{r1}(t) & \mathbf{e}_{r2}(t) & \cdots & \mathbf{e}_{rp}(t) \end{bmatrix} \tag{5.10}$$

In the preceding definition, the one norm of each element is:

$$\int_0^\infty |\mathbf{e}(t)|\,dt = \begin{bmatrix} \|\mathbf{e}_{11}(t)\|_1 & \|\mathbf{e}_{12}(t)\|_1 & \cdots & \|\mathbf{e}_{1p}(t)\|_1 \\ \|\mathbf{e}_{21}(t)\|_1 & \|\mathbf{e}_{22}(t)\|_1 & \cdots & \|\mathbf{e}_{2p}(t)\|_1 \\ \vdots & \vdots & \ddots & \vdots \\ \|\mathbf{e}_{r1}(t)\|_1 & \|\mathbf{e}_{r2}(t)\|_1 & \cdots & \|\mathbf{e}_{rp}(t)\|_1 \end{bmatrix} \tag{5.11}$$

and the approximation for (5.11) is:

$$\int_0^\infty |\mathbf{e}(t)|\,dt \simeq \begin{bmatrix} \sum_{n=0}^{\mathbf{N}} |\mathbf{e}_{11}^n|\,\Delta T & \sum_{n=0}^{\mathbf{N}} |\mathbf{e}_{12}^n|\,\Delta T & \cdots & \sum_{n=0}^{\mathbf{N}} |\mathbf{e}_{1p}^n|\,\Delta T \\ \sum_{n=0}^{\mathbf{N}} |\mathbf{e}_{21}^n|\,\Delta T & \sum_{n=0}^{\mathbf{N}} |\mathbf{e}_{22}^n|\,\Delta T & \cdots & \sum_{n=0}^{\mathbf{N}} |\mathbf{e}_{2p}^n|\,\Delta T \\ \vdots & \vdots & \ddots & \vdots \\ \sum_{n=0}^{\mathbf{N}} |\mathbf{e}_{r1}^n|\,\Delta T & \sum_{n=0}^{\mathbf{N}} |\mathbf{e}_{r2}^n|\,\Delta T & \cdots & \sum_{n=0}^{\mathbf{N}} |\mathbf{e}_{rp}^n|\,\Delta T \end{bmatrix} \tag{5.12}$$

Therefore the infinity norm of the error transfer function matrix is bounded by:

$$\|\mathbf{E}(j\omega)\|_\infty \lesssim \sigma_{\max}\left\{\begin{bmatrix} \sum_{n=0}^{N}|e_{11}^n|\,\Delta T & \sum_{n=0}^{N}|e_{12}^n|\,\Delta T & \cdots & \sum_{n=0}^{N}|e_{1p}^n|\,\Delta T \\ \sum_{n=0}^{N}|e_{21}^n|\,\Delta T & \sum_{n=0}^{N}|e_{22}^n|\,\Delta T & \cdots & \sum_{n=0}^{N}|e_{2p}^n|\,\Delta T \\ \vdots & \vdots & \ddots & \vdots \\ \sum_{n=0}^{N}|e_{r1}^n|\,\Delta T & \sum_{n=0}^{N}|e_{r2}^n|\,\Delta T & \cdots & \sum_{n=0}^{N}|e_{rp}^n|\,\Delta T \end{bmatrix}\right\} \tag{5.13}$$

and (5.13) is used to calculate the linearization error bound for a MIMO system.

The error analysis described above is based on the error in the unit impulse response. However, in general, the input for the nonlinear model is a step not an impulse; therefore, the impulse error must be derived from step response data. In the block diagram shown below, the setup for the error analysis is illustrated.

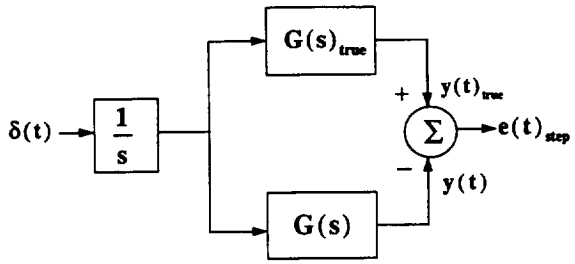

This block diagram can be rearranged so that the outputs of the transfer functions are the impulse responses.

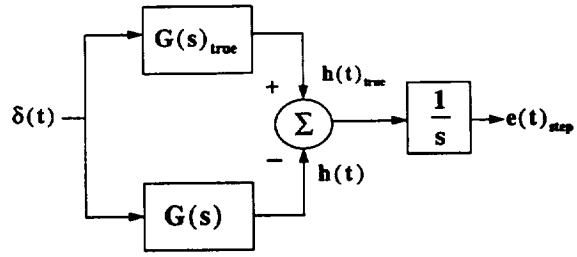

Now, the step error is represented as the integration of the impulse error. Therefore, the impulse response error can be determined from the step response data by taking the derivative of the step response error.

$$\mathbf{e}(t) = \frac{d}{dt}\left(y(t)_{true} - y(t)\right) \tag{5.14}$$

If the time derivative in the previous expression is approximated by a finite difference expression, then equation (5.14) can be rewritten as:

$$\mathbf{e}^n \simeq \left(\frac{\left(y_{true}^n - y_{true}^{n-1}\right) - \left(y^n - y^{n-1}\right)}{\Delta T}\right) \tag{5.15}$$

and the linearization error bound can be calculated using (5.13).

5.2 Model Reduction Error

When using the square root model reduction described in the previous section, the bound on the error between the linear full order model and the linear reduced order model can be quantified as shown below [17].

$$\|\mathbf{G}(j\omega) - \mathbf{G}_k(j\omega)\|_\infty \leqslant totbnd \tag{5.16}$$

The *totbnd* is defined as the following:

$$totbnd = 2 \sum_{i=k+1}^{m} \sigma_i \tag{5.17}$$

where, from equation (4.6), the σ are the Hankel singular values, k is the size of the reduced order model, and m is the number of nonzero Hankel singular values. The *totbnd* can also be used to determine the size of the reduced order model by using equation (5.16) and specifying an error tolerance that is to be satisfied over all frequencies. The size of the reduced order model is then equal to k with the *totbnd* equal to or less than the specified error tolerance.

5.3 Total Error Bound

As the infinity norm bound of a system is a Nyquist plane bound, the bounds serve as magnitudes of error incurred in each step in the modeling process. Thus, the total infinity norm bound is determined as the sum of the individual bounds from linearization and model reduction. This is represented as:

$$\|\mathbf{G}(j\omega)_{true} - \mathbf{G}_k(j\omega)\|_\infty \leqslant \|\mathbf{G}(j\omega)_{true} - \mathbf{G}(j\omega)\|_\infty + \|\mathbf{G}(j\omega) - \mathbf{G}_k(j\omega)\|_\infty \tag{5.18}$$

where $\mathbf{G}(j\omega)_{true}$ represents the transfer function of an exact linear model, $\mathbf{G}(j\omega)$ is the transfer function from the linearization process, and $\mathbf{G}_k(j\omega)$ is the transfer function from the model reduction process.

6 Example Application

6.1 Description

A mixed compression axisymmetric inlet is the model used to illustrate the CFD based linear modeling technique. This inlet is a good candidate because it is representative of an HSCT type inlet. The operating point is: $altitude = 65{,}000\ ft$, $p_\infty = 117.8\ \frac{lb}{ft^2}$, $T_\infty = 390\ ^\circ R$, $M_\infty = 2.35$, $M_{compressor\,face} \sim 0.4$ and $\gamma = 1.4$. Simulation data for the nonlinear model was obtained from the CFD code LAPIN [8]. The split-characteristics algorithm was chosen as the simulation method because of its accuracy; it is a conservative, shock-capturing method using characteristic information. The time step for the LAPIN simulations and for the linear model simulations was $\Delta t = 1 \times 10^{-4}$. Comparison of the transient simulation data, for calculation of the linearization error bound, was taken at every tenth data point from both sets of data.

Five different linear models were generated from a 41 node LAPIN CFD model of the inlet for five different system inputs. They included: a downstream corrected massflow perturbation, an upstream Mach number perturbation, an upstream static temperature perturbation, a downstream bypass massflow perturbation, and a throat bleed massflow perturbation. There is not an example of the downstream static pressure input because this is not representative of a real system input; it is used only for illustrative purposes. In addition, the downstream Mach number input does not have an example, because it is basically the same as the downstream corrected massflow input. The steady-state LAPIN data before the perturbation occurs is used to generate the linear model, and the linear model is validated from the transient LAPIN data that is

recorded after the perturbation. In general, the perturbation is a step input that is not too large so that the small perturbation analysis remains valid. The LAPIN model is a nonlinear system of 123 equations, and the linear full order model is a system of 123 equations. Note that the number of equations in the linear model is equal to the number states in the system. All of the reduced order models were calculated using the square root method with a specified error tolerance of 1.0×10^{-4}. This means that the *totbnd* will be equal to or less than 1.0×10^{-4} for the reduced order model. The nondimensional results for these examples are discussed in the next section, and the data for these matrices are listed in section 8.3 of the appendix.

6.2 Results

6.2.1 Downstream Corrected Massflow Perturbation

The inlet is perturbed at 0.07 seconds with a 1% step in downstream corrected massflow. The linear full order model has 123 states, one input, and four outputs. Figure 2 shows the output responses for the static pressure and total pressure at $X/R_c = 4.5016$ which is just after the normal shock (see Figure 1). The 1% change in the downstream corrected massflow produces a -2.1% change in steady state for the static pressure output and a -0.997% change in steady state for the total pressure output. Figure 3 shows the output responses for the static pressure and total pressure at $X/R_c = 5.6976$. The corresponding changes in the steady state values for the outputs are -1.325% for the static pressure and -0.997% for the total pressure. For this model the linearization error bound is $\|\mathbf{E}(j\omega)\|_\infty \lesssim 8.6090 \times 10^{-2}$. Figure 4 is a plot of the linear full order model eigenvalues and the linear reduced order model eigenvalues. The reduced order model has 18 states. The model reduction error bound is $\|\mathbf{G}(j\omega) - \mathbf{G}_k(j\omega)\|_\infty < 5.4184 \times 10^{-4}$, and the total error bound is 8.6632×10^{-2}.

6.2.2 Upstream Mach Number Perturbation

The inlet is perturbed at 0.05 seconds with a -2% step in upstream Mach number, and the downstream boundary condition is constant Mach number. The linear full order model has 123 states, one input, and six outputs. Figure 6 shows the output responses for the Mach number and total pressure at the cowl lip, $X/R_c = 2.0008$. The -2% change in the upstream Mach number produces a -2.02% change in steady state for the Mach number and a -7.07% change in steady state for the total pressure. Figure 7 shows the output responses for the Mach number and total pressure at the throat, $X/R_c = 3.8492$ (see Figure 5). The corresponding changes in the steady state values for the outputs are -9.83% for the Mach number and -7.07% for the total pressure. Figure 8 shows the static pressure and total pressure responses at $X/R_c = 5.154$ which is downstream of the normal shock. The corresponding changes in the steady state values for the outputs are -3.37% for the static pressure and -3.37% for the total pressure. The linearization error bound is $\|\mathbf{E}(j\omega)\|_\infty \lesssim 2.9309 \times 10^{-1}$. Figure 9 is a plot of the linear full order model eigenvalues and the linear reduced order model eigenvalues. The reduced order model has 29 states. The model reduction error bound is $\|\mathbf{G}(j\omega) - \mathbf{G}_k(j\omega)\|_\infty < 8.8679 \times 10^{-4}$, and the total error bound is 2.9398×10^{-1}.

6.2.3 Upstream Static Temperature Perturbation

The inlet is perturbed at 0.05 seconds with a 4% step in upstream static temperature, and the downstream boundary condition is constant Mach number. The linear full order model has 123 states, one input, and six outputs. Figure 11 shows the output responses for the Mach number and total pressure at the cowl lip, $X/R_c = 2.0008$. The 4% change in the upstream static temperature produces a -1.96% change in steady state for the Mach number and a -6.88% change in steady state for the total pressure. Figure 12 shows the output responses for the Mach number and total pressure at the throat, $X/R_c = 3.8492$ (see Figure 10). The corresponding changes in the steady state values for the outputs are -9.47% for the Mach

number and -6.89% for the total pressure. Figure 13 has the static pressure and total pressure responses at $X/R_c = 5.154$ which is downstream of the normal shock. The corresponding changes in the steady state values for the outputs are -3.27% for the static pressure and -3.27% for the total pressure. The linearization error bound is $\|\mathbf{E}(j\omega)\|_\infty \lesssim 1.4377 \times 10^{-1}$. Figure 14 is a plot of the linear full order model eigenvalues and the linear reduced order model eigenvalues. The reduced order model has 17 states. The model reduction error bound is $\|\mathbf{G}(j\omega) - \mathbf{G}_k(j\omega)\|_\infty < 7.7758 \times 10^{-4}$, and the total error bound is 1.4455×10^{-1}.

6.2.4 Downstream Bypass Massflow Perturbation

The inlet is perturbed at 0.1 seconds with a 200% step in downstream bypass massflow; this is equivalent to a 2% change in total massflow. The input is distributed over the bypass which is located at $X/R_c = 5.5131 - 6.0983$ and is downstream of the normal shock (see Figure 15). The downstream boundary condition is constant corrected massflow. The linear full order model has 123 states, one input, and six outputs. Figure 16 shows the static pressure and total pressure responses at $X/R_c = 4.5016$ which is before the bypass. The 200% change in the downstream bypass massflow produces a -3.88% change in steady state for the static pressure output and a -1.99% change in steady state for the total pressure output. Figure 17 shows the static pressure and total pressure responses in the bypass region at $X/R_c = 5.8063$. The corresponding changes in the steady state values for the outputs are -2.31% for the static pressure and -1.99% for the total pressure. Figure 18 shows the static pressure and total pressure responses after the bypass at $X/R_c = 6.2413$. The corresponding changes in the steady state values for the outputs are -1.99% for the static pressure and -1.99% for the total pressure. The linearization error bound is $\|\mathbf{E}(j\omega)\|_\infty \lesssim 1.801 \times 10^{-1}$. Figure 19 is a plot of the linear full order model eigenvalues and the linear reduced order model eigenvalues. The reduced order model has 22 states. The model reduction error bound is $\|\mathbf{G}(j\omega) - \mathbf{G}_k(j\omega)\|_\infty < 7.1382 \times 10^{-4}$, and the total error bound is 1.8081×10^{-1}.

6.2.5 Throat Bleed Massflow Perturbation

The inlet is perturbed at the first bleed on the cowl side of the inlet at 0.1 seconds with a 200% step in throat bleed massflow; this is equivalent to a 2% change in total massflow. The bleed is located on the cowl at $X/R_c = 3.205 - 3.625$ and is upstream of the normal shock (see Figure 20). The downstream boundary condition is constant corrected massflow. The linear full order model has 123 states, one input, and six outputs. Figure 21 shows the static pressure responses in the bleed region at $X/R_c = 3.3056$ and $X/R_c = 4.0667$. The 200% change in the throat bleed massflow produces a -1.28% change in steady state for the first static pressure output and a -5.89% change in steady state for the second static pressure output. Figure 22 shows the static pressure and total pressure responses at $X/R_c = 4.6103$ which is downstream of the normal shock. The corresponding changes in the steady state values for the outputs are -1.99% for the static pressure and -1.99% for the total pressure. Figure 23 shows the static pressure and total pressure responses at $X/R_c = 5.6976$. The corresponding changes in the steady state values for the outputs are -1.99% for the static pressure and -1.99% for the total pressure. The linearization error bound is $\|\mathbf{E}(j\omega)\|_\infty \lesssim 1.6266 \times 10^{-1}$. Figure 24 is a plot of the linear full order model eigenvalues and the linear reduced order model eigenvalues. The reduced order model has 30 states. The model reduction error bound is $\|\mathbf{G}(j\omega) - \mathbf{G}_k(j\omega)\|_\infty < 8.4574 \times 10^{-4}$, and the total error bound is 1.6351×10^{-1}.

6.3 Discussion

The error bounds for the linear models are all less than one, and most of the error is due to the linearization process. The specific causes and importance of the linearization error have not yet been determined. Certainly, some of the linearization error can be attributed to the fact that we are modeling a nonlinear system with a linear model, and there will always be inherently some amount of error. However, the linearization error can most likely be attributed to inaccuracies in the linear modeling process. The identification of

the causes and minimization of the linearization error will be addressed at a later date.

In general, a linear model with multiple inputs and outputs is more controllable and observable than a linear model with fewer inputs and outputs. Therefore, the reduced order model for a multi-input/multi-output model will be larger than for a single-input/single-output model. In addition, models with distributed inputs, such as the downstream bypass and throat bleed, have larger reduced order models, because they have more entries in the input matrix which increases the controllability of the system. Note that in the plots of the full order model eigenvalues and reduced order eigenvalues, the full order model eigenvalues closest to the origin are reproduced in the reduced order model. But the full order model eigenvalues farther away from the origin are approximated by just a few eigenvalues in the reduced order model.

The size of the reduced order model is dependent upon the error tolerance that is used. If the error tolerance is less restrictive, the full order model can be further reduced as shown in the following table.

Model	Error Tolerance	ROM Error Bound	Size ROM	Error Tolerance	ROM Error Bound	Size ROM	Percent ROM Further Reduced
1	1×10^{-3}	5.4184×10^{-4}	18	1×10^{-2}	5.0708×10^{-3}	16	11.1
2	1×10^{-3}	8.8679×10^{-4}	29	1×10^{-2}	8.1463×10^{-3}	24	17.2
3	1×10^{-3}	7.7758×10^{-4}	17	1×10^{-2}	6.9055×10^{-3}	14	17.6
4	1×10^{-3}	7.1382×10^{-4}	22	1×10^{-2}	3.7714×10^{-3}	20	9.1
5	1×10^{-3}	8.4574×10^{-4}	30	1×10^{-2}	7.7581×10^{-3}	26	16.7

In Figure 25 the size of the reduced order model is shown for error tolerances greater than or equal to 1.0×10^{-4}.

7 Conclusion

CFD models provide accurate models of internal fluid flows. In order to do this, many dynamic states are necessary. Unfortunately, the control engineer is somewhat at a loss as to what to do with all of this information, particularly in designing a controller for a plant of this size. But as was shown, it is possible to extract information from CFD results and model the propulsion system using linearized CFD equations. This method provides a small perturbation model that can be used for control applications and real-time simulations. It is important to note the utility of the modeling procedure; all that is needed to obtain a linear model of the propulsion system is the spatial step and steady-state operating conditions from a CFD simulation or experiment. This research represents a beginning step in establishing a bridge between the controls discipline and the CFD discipline so that the control engineer is able to effectively use CFD results in control system design and analysis. In the future this research will be applied to multi-dimensional flows and viscous flows.

8 Appendices

8.1 Symbols

A	cross sectional area (ft^2)
B_{bc}	physical boundary condition
c	speed of sound $\left(\frac{ft}{sec}\right)$
E	total energy per unit mass $\left(\frac{lb\,ft}{slug}\right)$
$\mathbf{E}$	error transfer function matrix
e	internal energy per unit mass $\left(\frac{ft^2}{sec^2}\right)$
$\mathbf{e}$	error
F	flux vector
F_S	mass transfer momentum term
G	area source vector
$\mathbf{G}$	transfer function
$\mathbf{g}$	impulse response
H	total enthalpy per unit mass
J	Jacobian
K	matrix of right eigenvectors
M	Mach number
M_S	mass transfer continuity term
m	massflow per unit area $\left(\frac{slug}{sec\ ft^2}\right)$
$\dot{m}$	massflow $\left(\frac{slug}{sec}\right)$
p	pressure $\left(\frac{lb}{ft^2}\right)$
P	controllability Grammian
Q	observability Grammian
Q_S	mass transfer energy term
R	universal gas constant
R_c	cowl radius (ft)
s	entropy
t	time (sec)
u	velocity $\left(\frac{ft}{sec}\right)$
$\vec{u}$	vector of conservative variables
$\vec{w}$	vector of characteristic variables
x	distance (ft)

8.1.1 Greek Symbols

ΔT	sampling time (sec)
Δx	spatial step (ft)
ε	$\varepsilon = \rho E$, total energy per unit volume $\left(\frac{lb\,ft}{ft^3}\right)$
δ	small perturbation variable
γ	ratio of specific heats
Λ	diagonal matrix of local characteristics
λ	eigenvalue
ρ	density $\left(\frac{slug}{ft^3}\right)$
σ	singular value
ω	frequency $\left(\frac{rad}{sec}\right)$

8.1.2 Subscripts

bc	boundary condition
c	corrected
i	grid point
k	size of reduced order model
L	left
N	total number of grid points
p	number of outputs
R	right
r	number of inputs
S	source
sl	sea level conditions
ss	steady-state
t	total conditions

8.1.3 Superscripts

N	numerical
n	time level
P	physical
T	transpose

8.2 Figures

8.2.1 Example #1: Downstream Corrected Massflow Perturbation

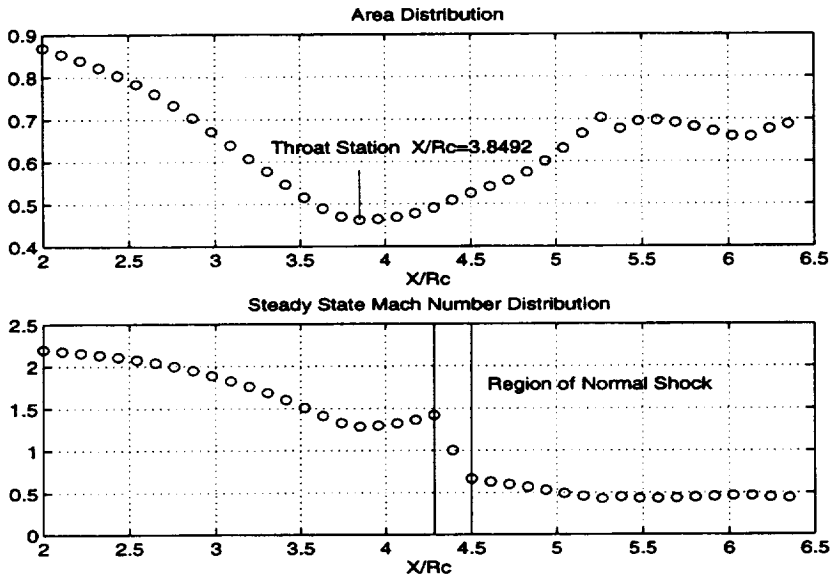

Figure 1: Steady State Operating Point

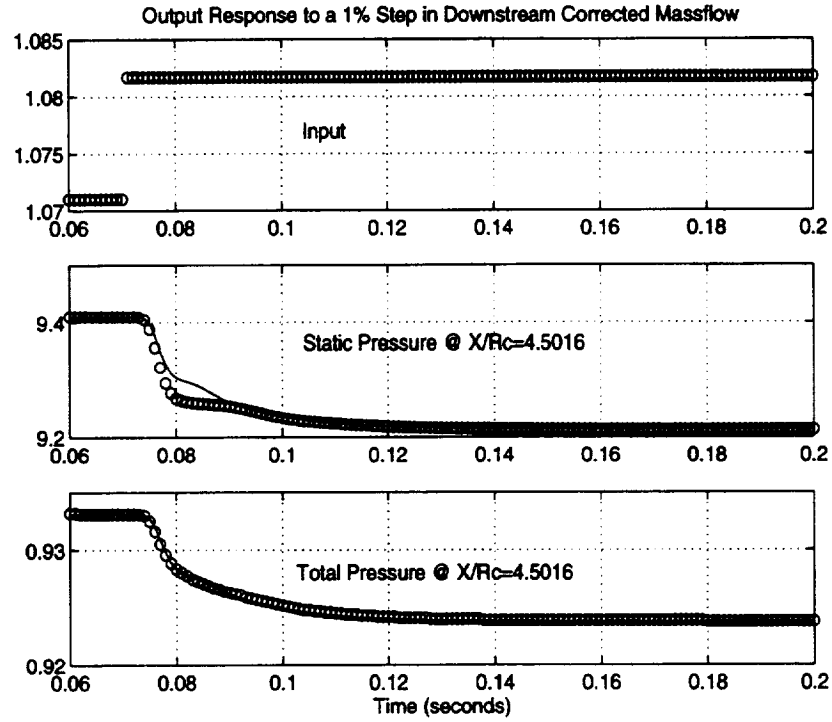

Figure 2: o Lapin Results/- Linear ROM Results

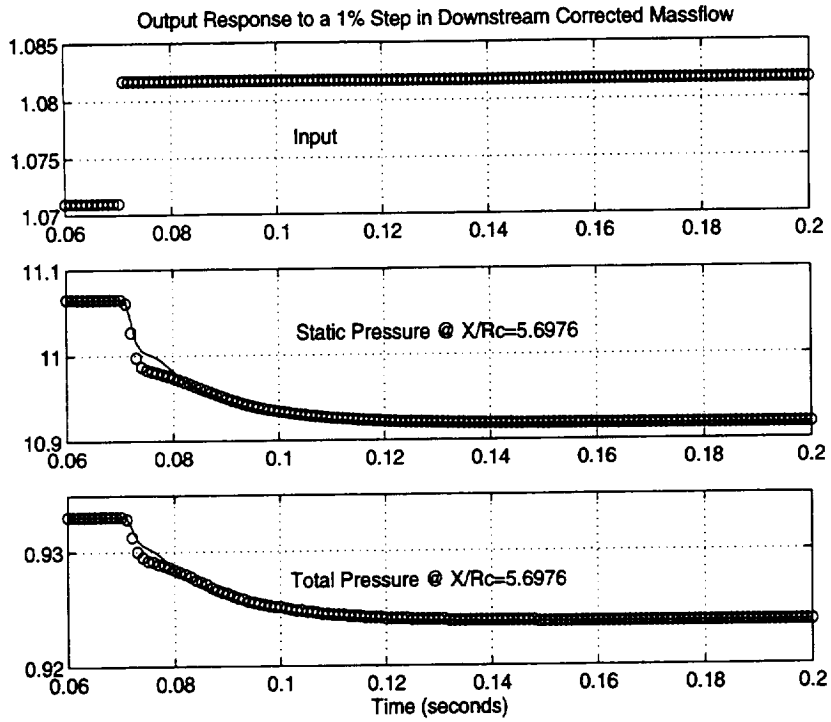

Figure 3: o LAPIN Results/- Linear ROM Results

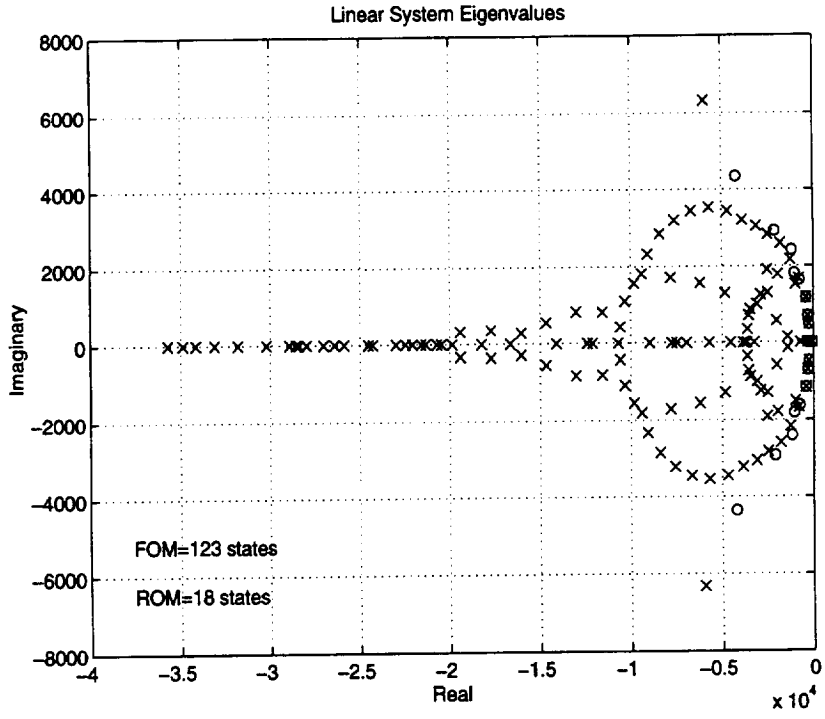

Figure 4: x FOM Eigenvalues/o ROM Eigenvalues

8.2.2 Example #2: Upstream Mach Number Perturbation

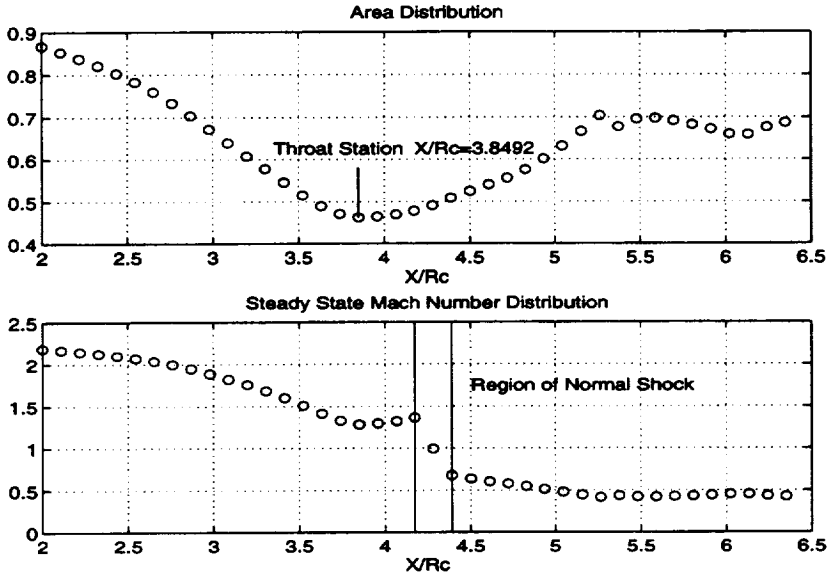

Figure 5: Steady State Operating Point

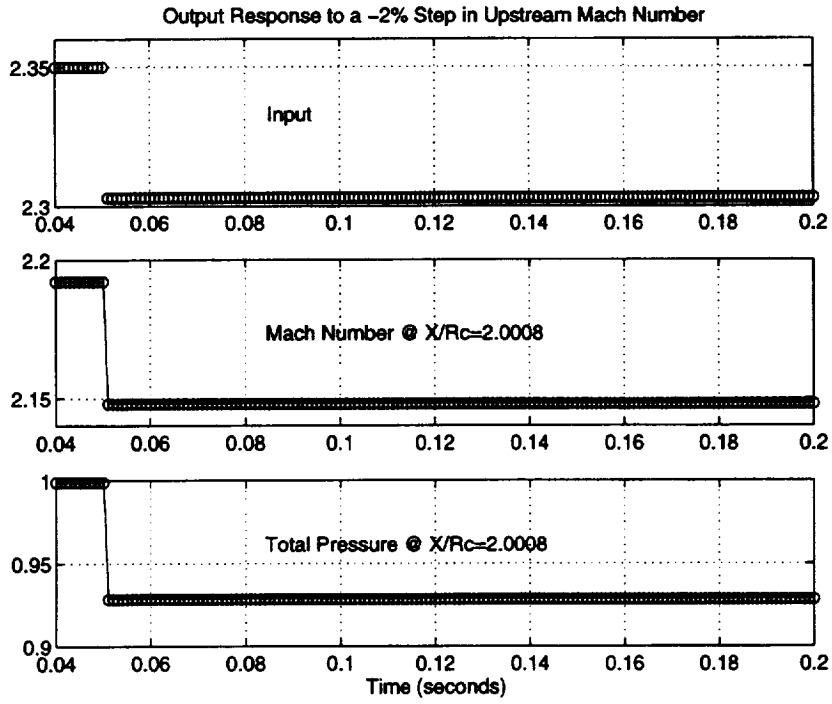

Figure 6: o LAPIN Results/- Linear ROM Results

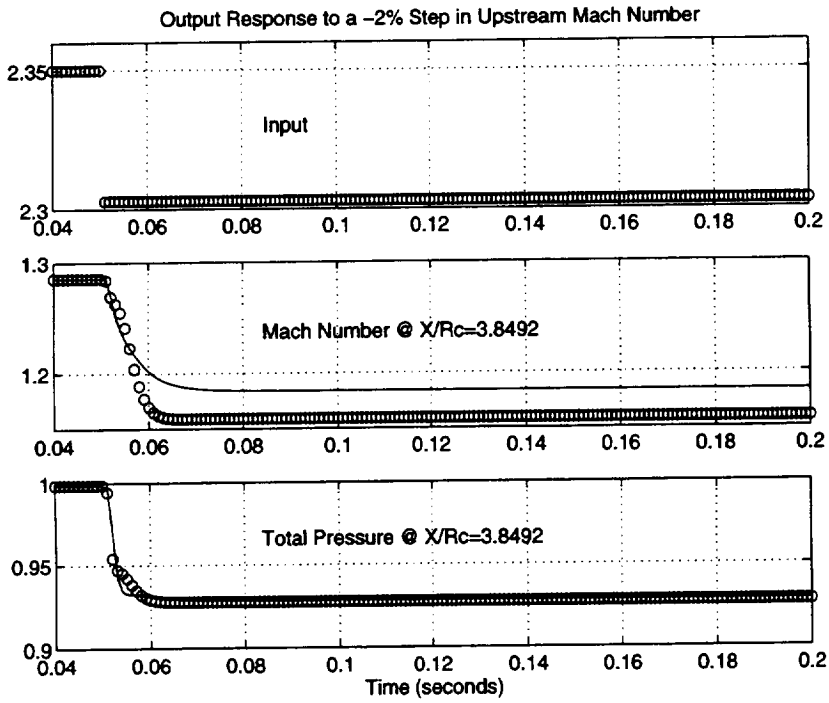

Figure 7: o LAPIN Results/- Linear ROM Results

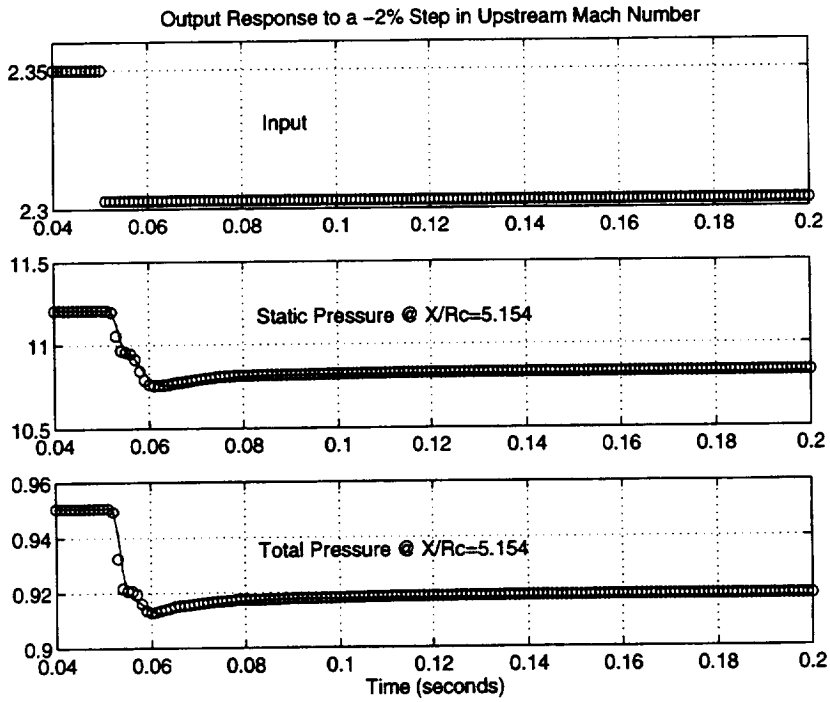

Figure 8: o LAPIN Results/- Linear ROM Results

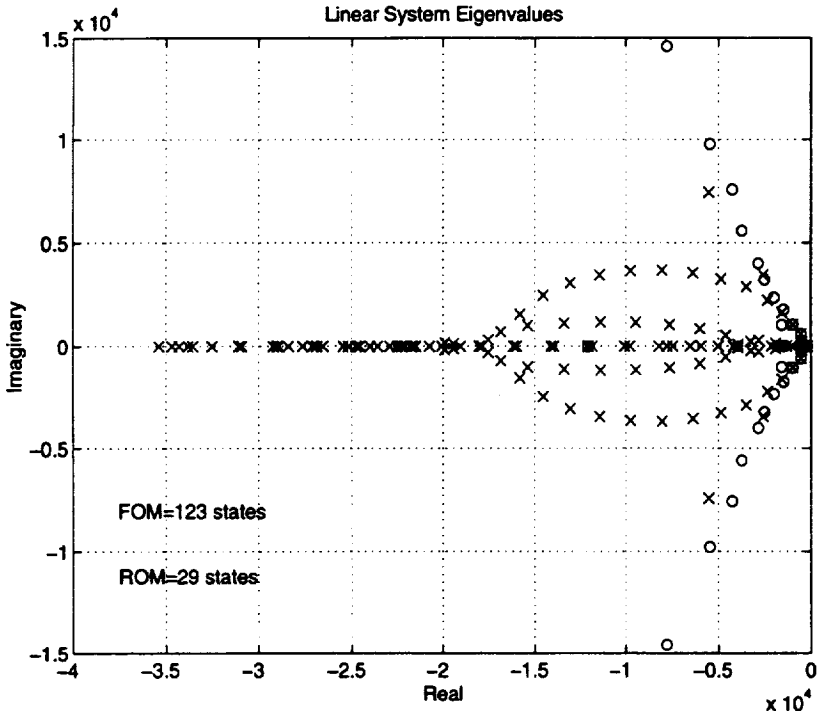

Figure 9: x FOM Eigenvalues/o ROM Eigenvalues

8.2.3 Example #3: Upstream Static Temperature Perturbation

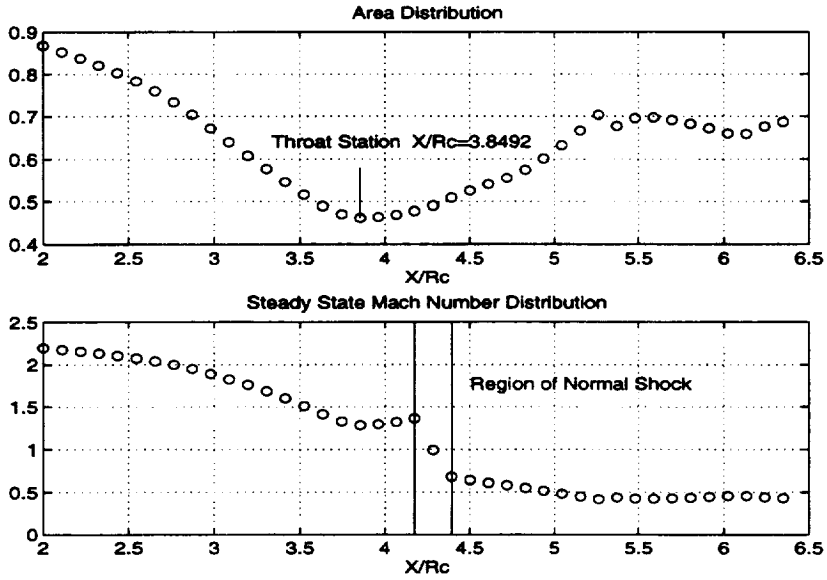

Figure 10: Steady State Operating Point

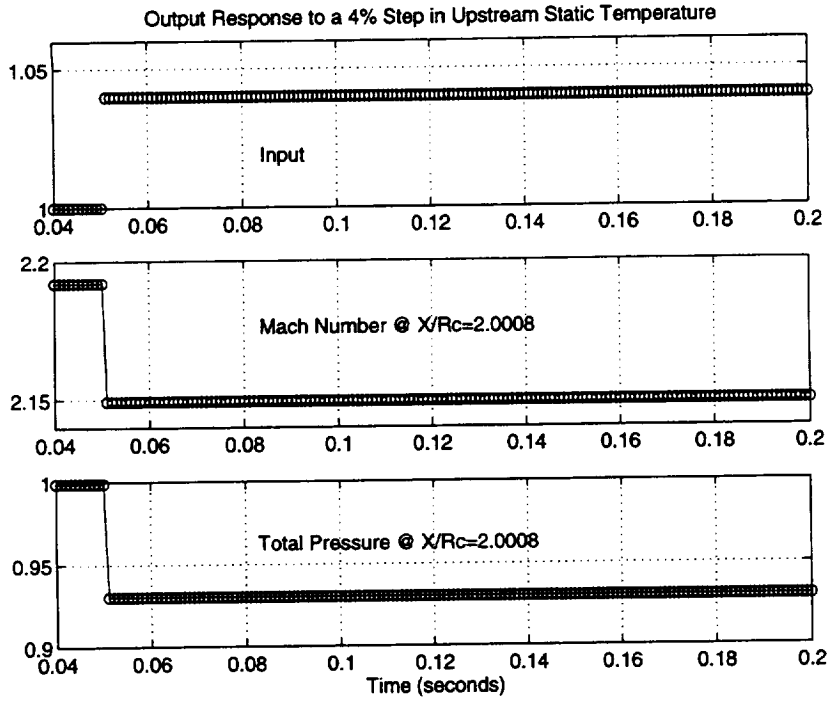

Figure 11: o LAPIN Results/- Linear ROM Results

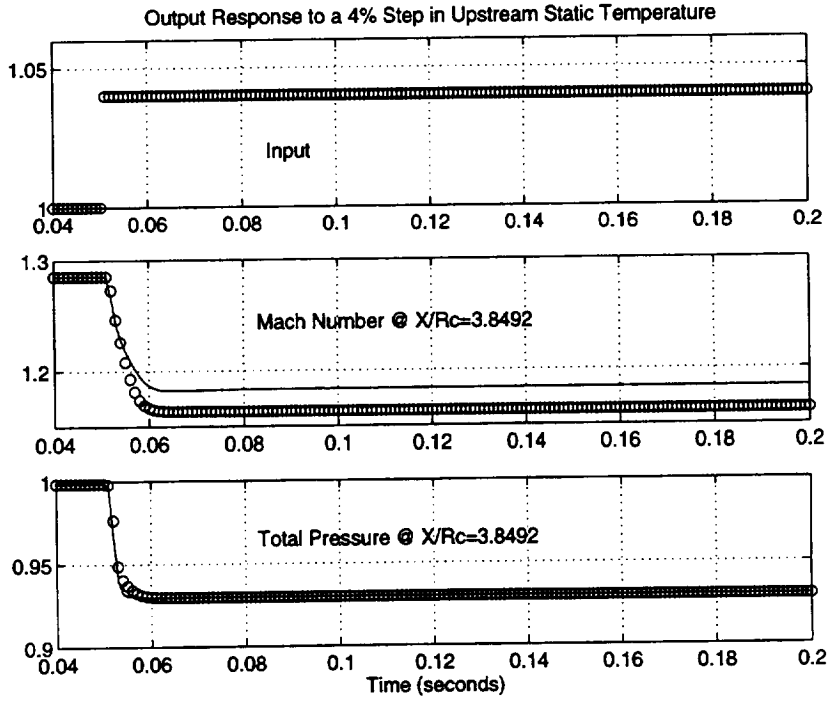

Figure 12: o LAPIN Results/- Linear ROM Results

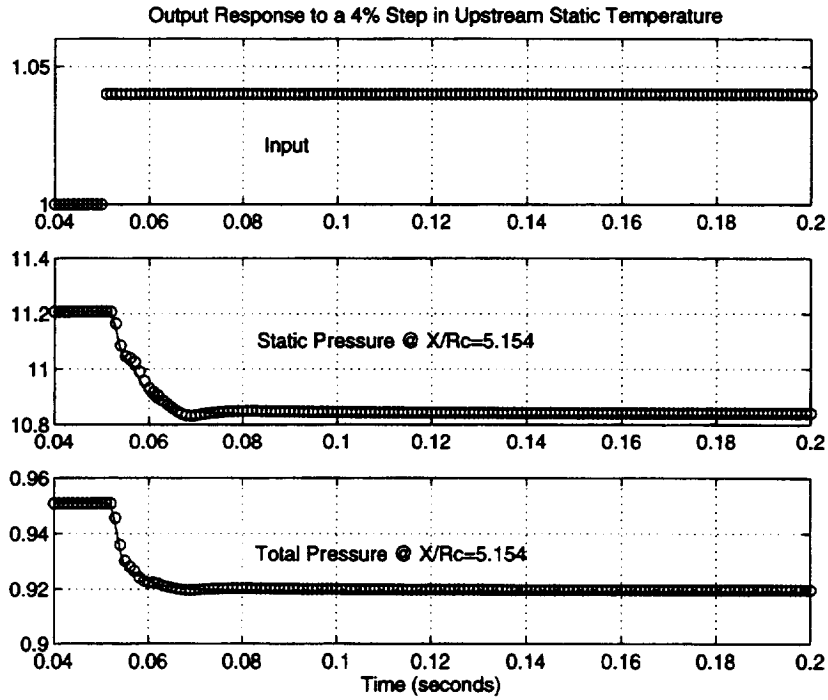

Figure 13: o LAPIN Results/- Linear ROM Results

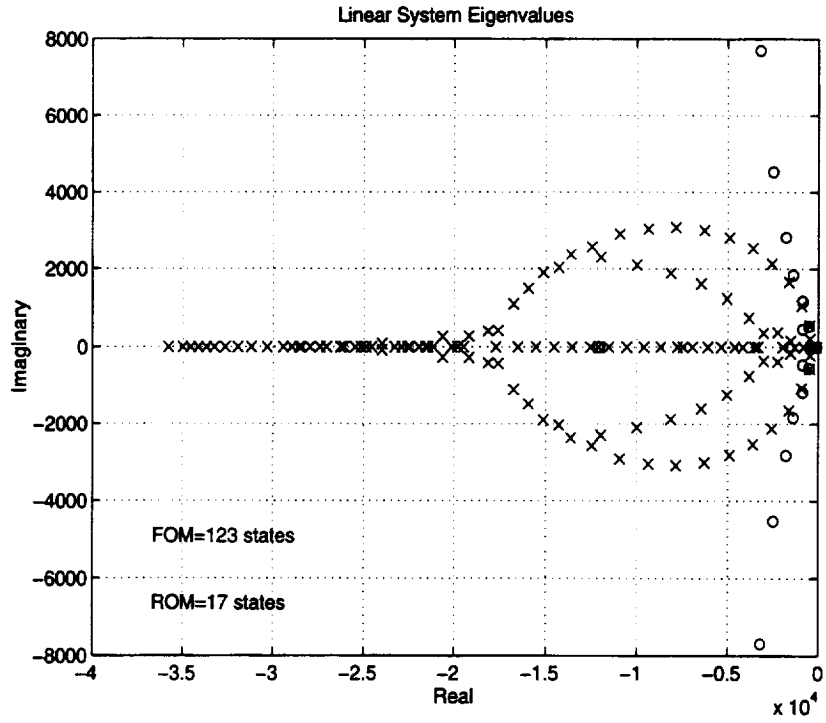

Figure 14: x FOM Eigenvalues/o ROM Eigenvalues

8.2.4 Example #4: Downstream Bypass Massflow Perturbation

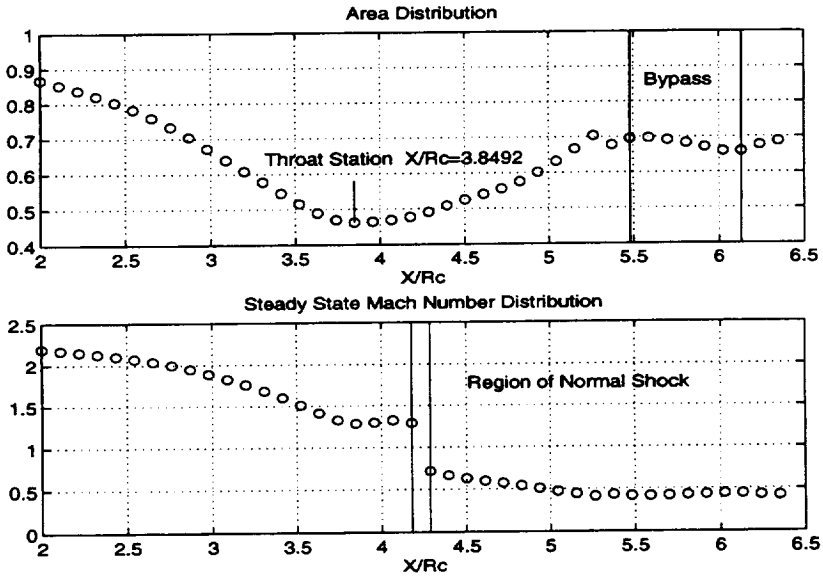

Figure 15: Steady State Operating Point

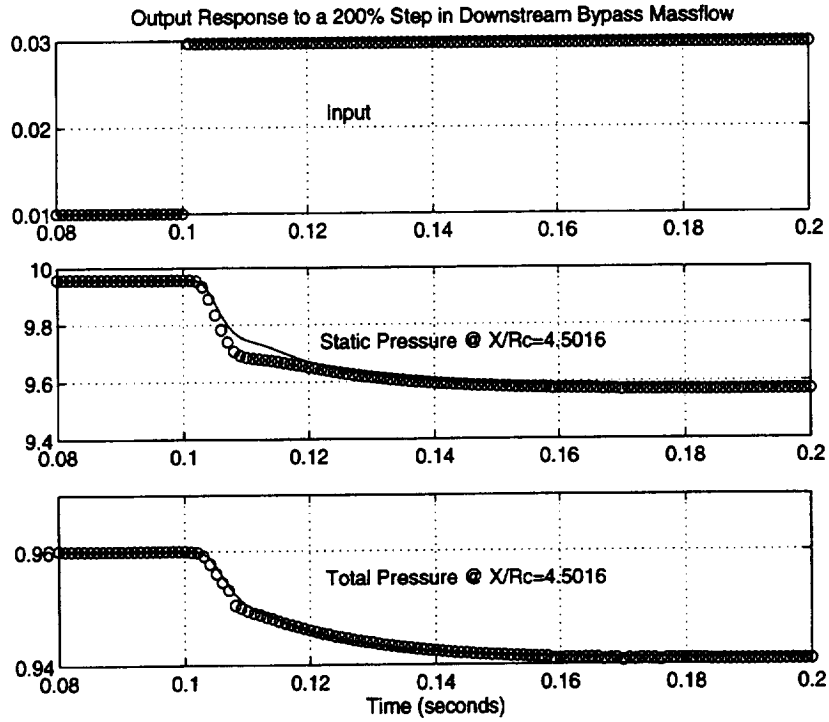

Figure 16: o LAPIN Results/- Linear ROM Results

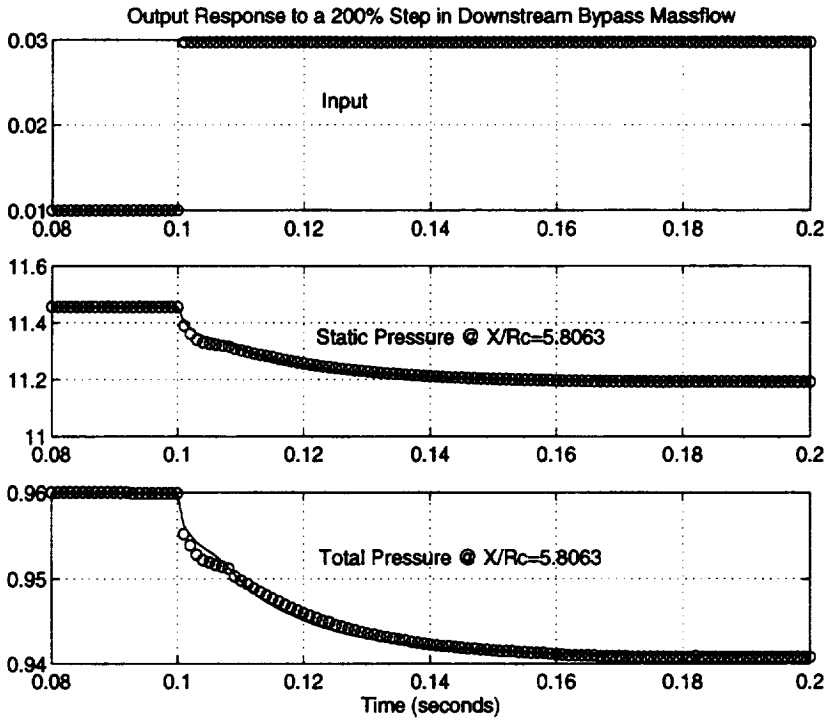

Figure 17: o LAPIN Results/- Linear ROM Results

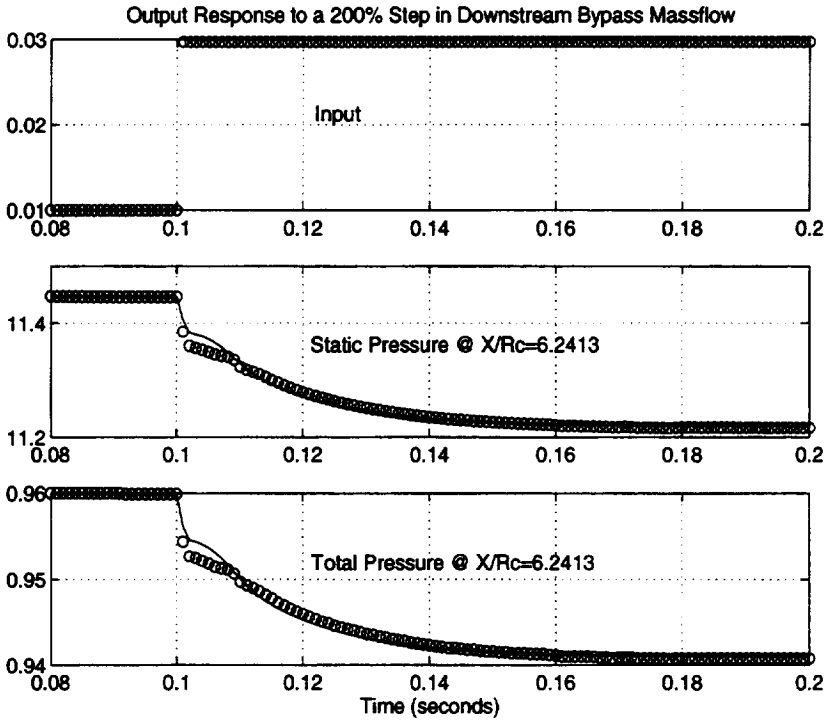

Figure 18: o LAPIN Results/- Linear ROM Results

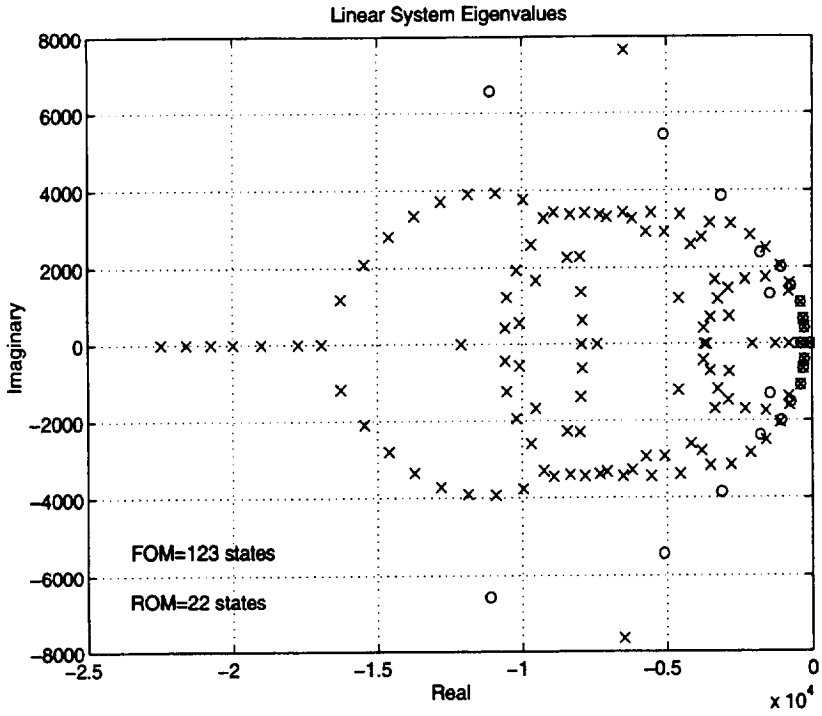

Figure 19: x FOM Eigenvalues/o ROM Eigenvalues

8.2.5 Example #5: Throat Bleed Massflow Perturbation

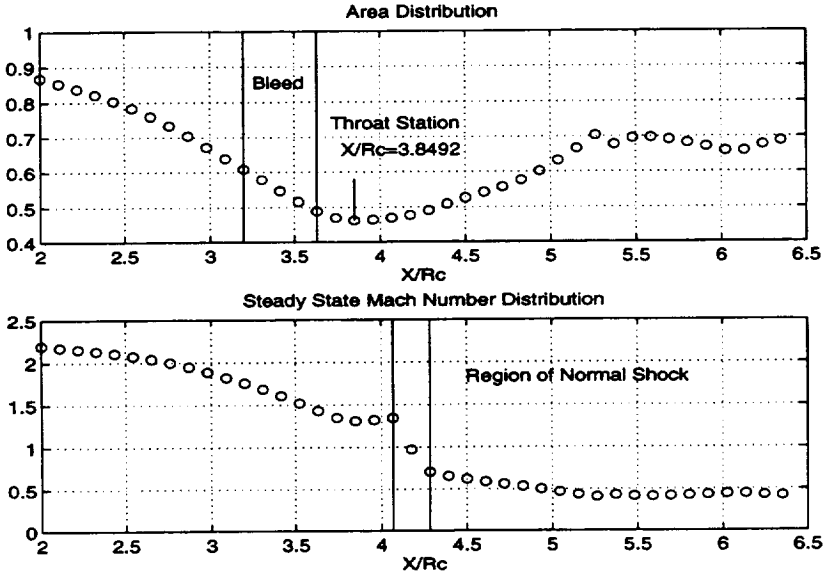

Figure 20: Steady State Operating Point

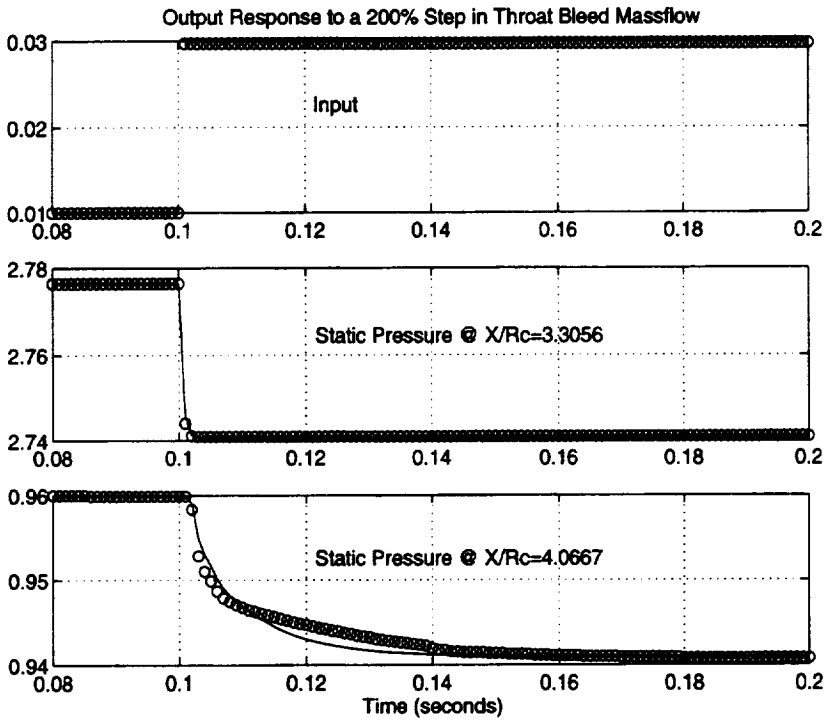

Figure 21: o LAPIN Results/- Linear ROM Results

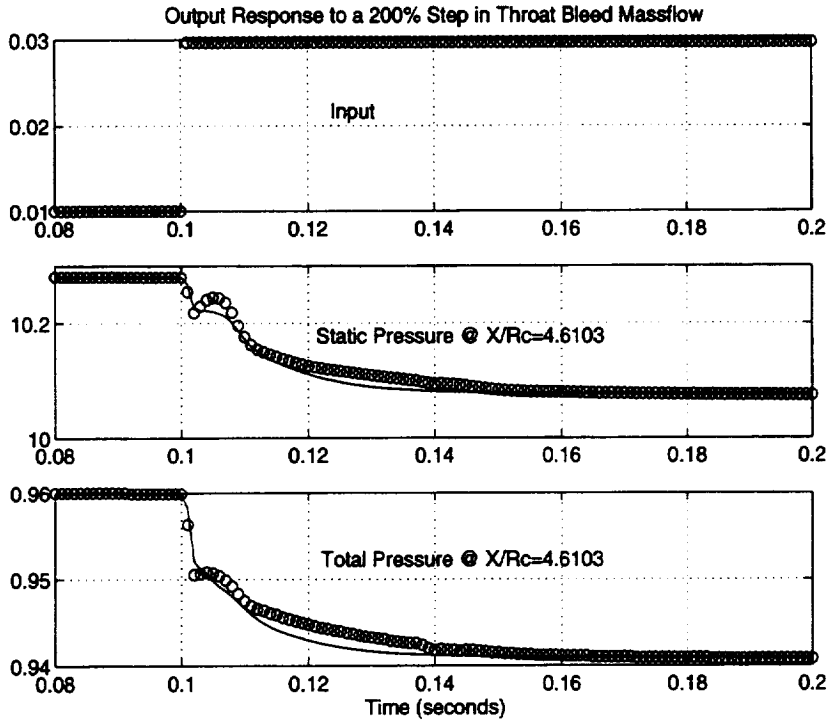

Figure 22: o LAPIN Results/- Linear ROM Results

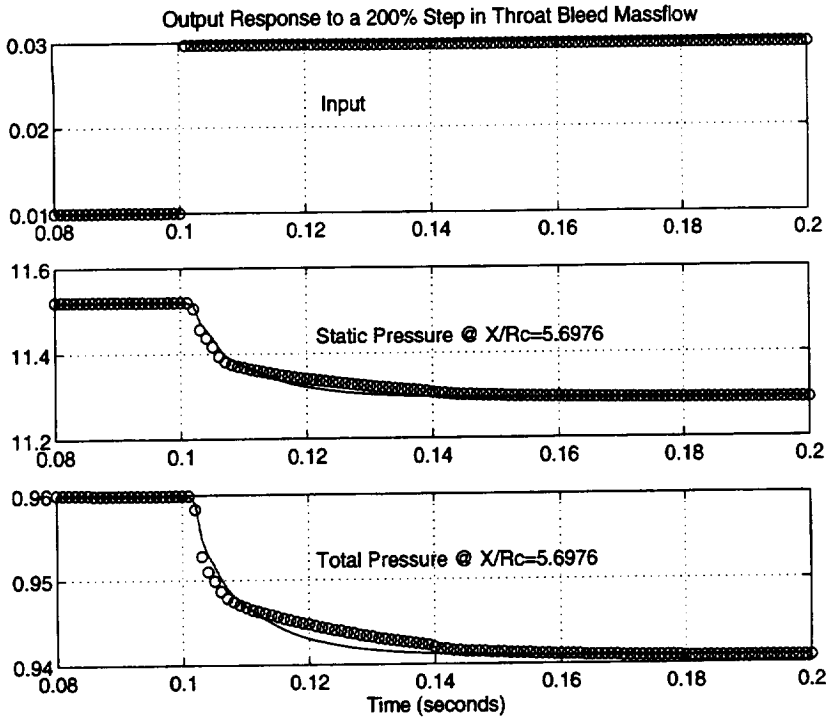

Figure 23: o LAPIN Results/- Linear ROM Results

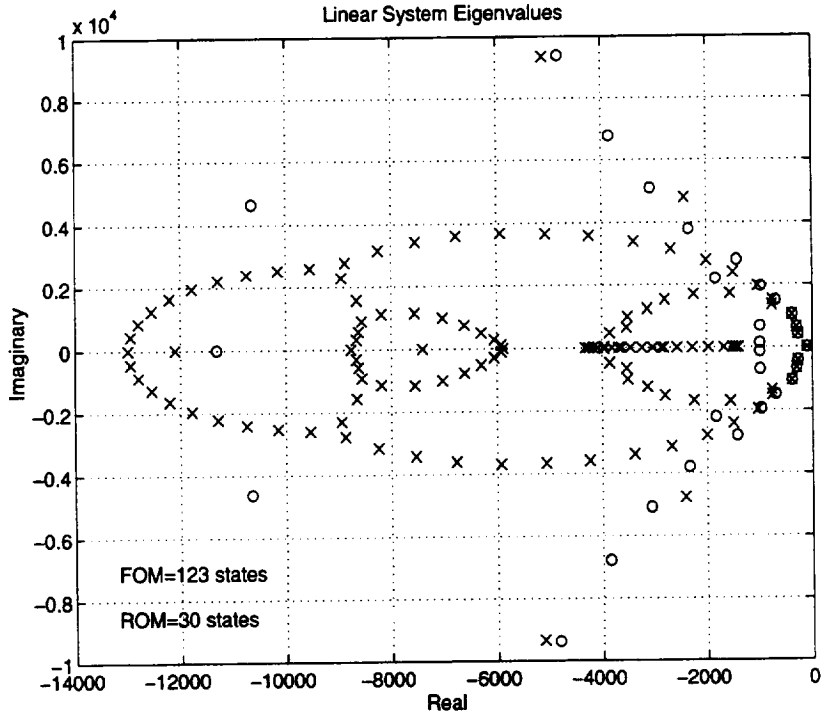

Figure 24: x FOM Eigenvalues/o ROM Eigenvalues

Model	Description
1	Corrected Massflow Downstream Perturbation
2	Mach Number Upstream Perturbation
3	Static Temperature Upstream Perturbation
4	Bypass Massflow Downstream Perturbation
5	Throat Bleed Massflow Perturbation

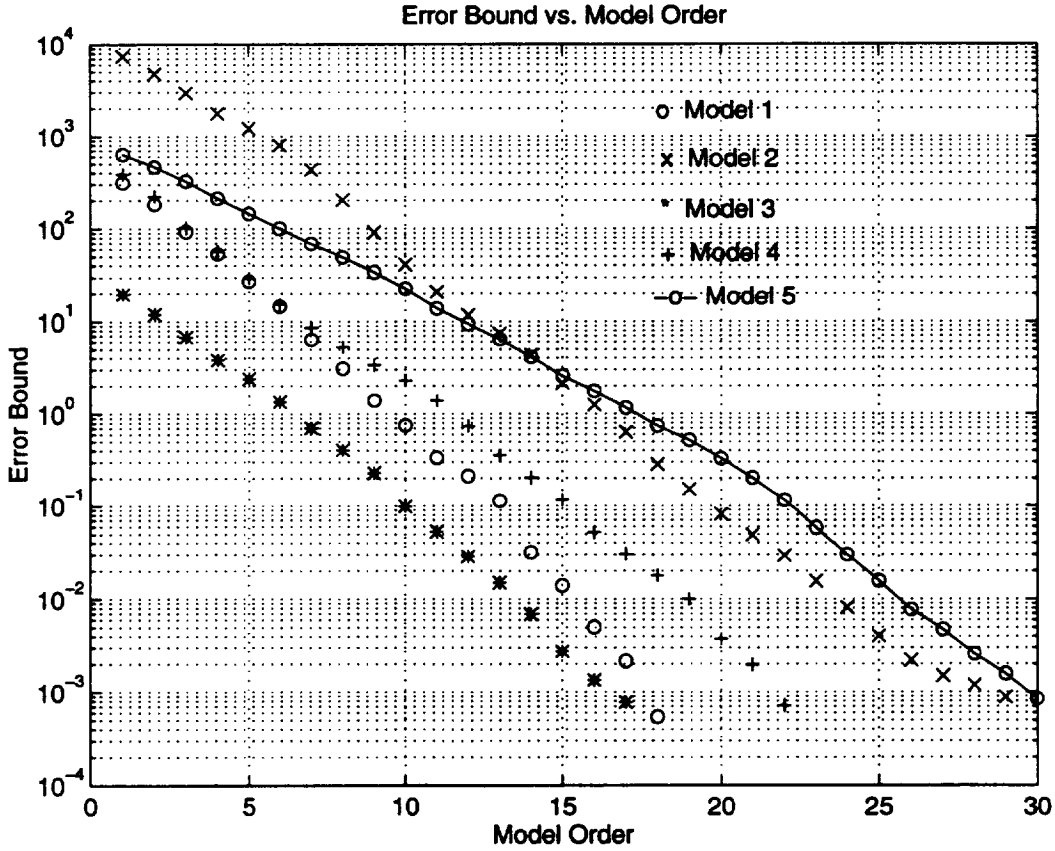

Figure 25: Model Reduction Error Bound, $\|\mathbf{G}(j\omega) - \mathbf{G}_k(j\omega)\|_\infty$ vs. Model Order

8.3 Matrices for Reduced Order Linear Models

8.3.1 Example #1: Downstream Corrected Massflow Perturbation

System Matrix (A)

Columns 1 through 8

-5.0531e+001	9.5982e+001	-3.5473e+000	1.3863e+002	-2.9821e+001	-5.0993e+001	5.8175e+000	2.3776e+001
-1.3626e+002	-1.0095e+002	6.3264e+002	1.2554e+001	1.1256e+001	8.9664e+001	1.1838e+002	-2.2555e+001
-9.7600e+001	-6.3349e+002	-1.6514e+002	3.2995e+002	6.4698e+001	-7.8829e+001	-2.3237e+002	2.8694e+001
-1.3978e+002	-2.6393e+002	-5.5567e+002	-5.5770e+002	1.0581e+003	7.1162e+002	-2.9082e+002	-2.4638e+002
-4.3700e+001	-1.0115e+002	-1.7381e+002	-1.1128e+003	-1.2396e+002	4.5799e+001	2.6706e+001	1.0699e+002
-5.6857e+001	-1.3494e+002	-1.8618e+002	-7.7058e+002	-3.3903e+002	-4.0770e+002	-1.2495e+003	1.9337e+002
6.9266e+001	1.4126e+002	2.5384e+002	6.9625e+002	3.6377e+002	1.7520e+003	-8.8929e+002	3.6164e+002
2.7289e+001	5.9506e+001	9.1176e+001	2.7323e+002	1.3399e+002	3.3066e+002	-8.5320e+002	-3.4361e+002
4.4890e+001	9.6489e+001	1.4822e+002	4.0073e+002	2.5359e+002	6.4170e+002	-1.4092e+003	-1.8542e+003
-2.1792e+001	-4.6514e+001	-7.2873e+001	-1.9672e+002	-1.1834e+002	-3.1405e+002	5.7460e+002	6.4780e+002
-1.1872e+001	-2.5356e+001	-3.9857e+001	-1.0912e+002	-6.2969e+001	-1.6572e+002	2.9735e+002	2.8598e+002
-9.7418e+000	-2.0860e+001	-3.2614e+001	-8.9653e+001	-5.2085e+001	-1.3348e+002	2.4994e+002	2.3515e+002
-4.9799e+000	-1.0657e+001	-1.6681e+001	-4.5779e+001	-2.6666e+001	-6.8414e+001	1.2701e+002	1.2231e+002
-1.2458e+001	-2.6654e+001	-4.1741e+001	-1.1448e+002	-6.6654e+001	-1.7167e+002	3.1684e+002	3.0743e+002
4.0538e+000	8.6723e+000	1.3577e+001	3.7188e+001	2.1727e+001	5.6021e+001	-1.0368e+002	-1.0106e+002
-2.8534e+000	-6.1049e+000	-9.5543e+000	-2.6170e+001	-1.5300e+001	-3.9431e+001	7.3161e+001	7.1255e+001

Columns 9 through 16

-2.2737e+001	1.8558e+001	-5.6151e-001	-9.3027e+000	-3.6632e+000	-8.7882e+000	1.7251e-001	1.5208e+000
-5.6275e+001	-5.2772e+000	-1.4529e+001	1.0189e+001	2.1825e-001	-8.3295e+000	6.7160e+000	2.4559e+000
8.8503e+001	4.3909e+000	2.0754e+001	-1.4385e+001	1.0706e+000	1.6390e+001	-1.0664e+001	-4.2498e+000
2.3392e+002	-1.7316e+002	1.9630e+001	8.4251e+001	3.5265e+001	8.8130e+001	-6.6380e+000	-1.5776e+001
-2.0954e+002	6.9117e+001	-4.1769e+001	-3.3951e+001	-9.7271e+000	-4.5608e+001	6.6752e+000	1.1915e+001
-1.7650e+002	2.6776e+002	5.0634e+001	-1.2444e+002	-5.3266e+001	-7.7962e+001	-5.2442e+000	6.3780e+000
1.2684e+003	-2.1804e+002	1.3182e+002	-1.7335e+001	4.9232e+001	2.3697e+002	-8.2795e+001	-5.2819e+001
1.4535e+003	-5.3995e+002	8.0170e+001	2.1637e+002	6.5040e+001	1.3713e+002	-1.2079e+001	-2.8489e+001
-1.7878e+003	2.8002e+002	-9.1096e+002	-3.2649e+002	-2.1113e+002	-9.3829e+002	2.1521e+002	2.0857e+002
1.6300e+003	-1.0998e+003	1.6978e+003	1.0967e+003	5.7465e+002	1.0197e+003	-2.0043e+002	-9.8592e+001
1.1766e+003	-2.3087e+003	-5.0197e+002	1.9474e+002	1.0150e+002	-6.0311e+001	2.0951e+002	1.1137e+002
8.0209e+002	-1.1925e+003	-8.8040e+002	-1.1691e+003	2.3093e+002	8.7987e+002	-8.3132e+001	2.5913e+002
4.1033e+002	-5.9207e+002	-4.4511e+002	-1.3832e+003	-3.7488e+002	9.3536e+002	2.1132e+002	1.6773e+002
1.0412e+003	-1.3899e+003	-1.0419e+003	-3.5831e+003	-2.6502e+003	-2.8327e+003	4.5691e+002	1.3217e+003
-3.2606e+002	4.1539e+002	3.3400e+002	9.8463e+002	5.7259e+002	1.7450e+003	-1.3960e+003	-2.2212e+003
2.2679e+002	-2.8714e+002	-2.4366e+002	-7.0375e+002	-4.4473e+002	-1.4424e+003	3.1002e+003	-1.3535e+003

```
Input Matrix (B)

 -1.2349e+002
 -1.1531e+002
 -1.2052e+002
 -1.4858e+002
 -5.6508e+001
 -7.2107e+001
  8.4827e+001
  3.3662e+001
  5.4698e+001
 -2.6579e+001
 -1.4507e+001
 -1.1908e+001
 -6.0864e+000
 -1.5226e+001
  4.9534e+000
 -3.4865e+000

Output Matrix (C)

  Columns 1 through 6
  7.2912e+001 -9.4400e+001  9.0049e+001 -7.0459e+001 -3.4989e+000  5.7198e+001
  4.3923e+001 -5.0680e+001  6.0438e+001 -5.2065e+001  2.7107e+001  2.3553e+001
  7.1449e+001  4.0608e+001 -5.0521e+001 -9.8690e+001  2.6106e+001  3.6828e+001
  5.3845e+001  1.2970e+001 -1.4544e+001 -6.8271e+001  4.2007e+001  4.0985e+000

  Columns 7 through 12
  3.9146e+001 -9.8341e+000 -1.5696e+001 -9.5358e+000 -1.0995e+001  6.7652e+000
  3.8255e+001 -2.4920e+001 -2.6217e+000 -8.3792e+000  6.4659e+000  6.6546e+000
 -5.8219e+001 -1.5616e+001  3.8035e+001 -2.3322e+001  4.5375e+000  6.7151e+000
 -2.8467e+001 -1.3098e+001  3.5944e+001 -1.1805e+000  5.2130e+000  2.5809e+000

  Columns 13 through 16
  2.2411e+000  2.1395e+000  2.9905e+000  2.8638e-001
  4.4775e-001 -3.2950e+000  1.5944e-001  6.0509e-001
  5.6116e+000  1.1445e+001 -3.9104e+000 -1.5943e+000
 -5.7590e-001  9.2404e+000  5.2518e-001 -3.0275e+000


Input/Output Matrix (D)

     0
     0
     0
     0
```

8.3.2 Example #2: Upstream Mach Number Perturbation

System Matrix (A)

Columns 1 through 8

-4.7989e+002	-8.0461e+002	1.1919e+003	4.4789e+002	-3.2507e+001	-1.2974e+001	1.3684e+001	-2.8930e+001
-2.3966e+003	-7.0292e+003	3.5544e+003	1.8038e+003	6.0480e+002	6.5190e+002	3.9329e+002	2.6561e+002
1.2925e+003	6.3020e+003	-3.9460e+003	-7.2008e+002	7.8241e+001	-1.3056e+002	-1.7082e+002	1.0180e+002
7.0145e+002	3.2021e+003	-3.1453e+003	-1.2792e+003	2.6425e+002	6.8606e+002	4.4057e+002	-1.6357e+002
3.1233e+002	1.3697e+003	-1.3704e+003	-1.0774e+003	-3.8311e+002	2.8537e+002	-1.3389e+001	-1.8111e+002
4.2236e+002	1.9406e+003	-1.8110e+003	-1.5467e+003	-1.2638e+003	-9.4211e+002	1.9943e+002	6.5441e+002
2.7045e+002	1.2635e+003	-1.1531e+003	-9.7864e+002	-6.6649e+002	-1.3913e+003	-4.4465e+002	6.2082e+002
1.9155e+002	8.9874e+002	-8.4329e+002	-5.5662e+002	-3.9635e+002	-1.2119e+003	-1.0113e+003	-3.4680e+002
2.7360e+002	1.3390e+003	-1.1968e+003	-8.1413e+002	-7.9517e+002	-1.5803e+003	-1.2496e+003	-1.3060e+003
-2.1025e+002	-1.0269e+003	9.1585e+002	6.5927e+002	5.5239e+002	9.7963e+002	6.8811e+002	9.3371e+002
-1.1213e+002	-5.4295e+002	4.9006e+002	3.4843e+002	2.7545e+002	4.8306e+002	3.6034e+002	4.1320e+002
-1.1701e+002	-5.6701e+002	5.1173e+002	3.6188e+002	2.8691e+002	5.2118e+002	3.8128e+002	4.1158e+002
-2.7688e+001	-1.3441e+002	1.2102e+002	8.5782e+001	6.9247e+001	1.2405e+002	9.1122e+001	1.0242e+002
-2.7055e+001	-1.3128e+002	1.1825e+002	8.3912e+001	6.7285e+001	1.2040e+002	8.8197e+001	9.9594e+001
-5.5791e+001	-2.7080e+002	2.4384e+002	1.7297e+002	1.3899e+002	2.4960e+002	1.8233e+002	2.0535e+002
3.3644e+001	1.6328e+002	-1.4707e+002	-1.0420e+002	-8.3744e+001	-1.5085e+002	-1.1037e+002	-1.2284e+002
2.4625e+001	1.1950e+002	-1.0765e+002	-7.6266e+001	-6.1252e+001	-1.1029e+002	-8.0737e+001	-8.9809e+001
1.3642e+001	6.6201e+001	-5.9631e+001	-4.2266e+001	-3.3932e+001	-6.1050e+001	-4.4652e+001	-4.9862e+001
-1.9742e+001	-9.5800e+001	8.6300e+001	6.1162e+001	4.9083e+001	8.8315e+001	6.4619e+001	7.2065e+001
8.9452e+000	4.3407e+001	-3.9102e+001	-2.7712e+001	-2.2241e+001	-4.0024e+001	-2.9282e+001	-3.2653e+001
3.5494e+000	1.7224e+001	-1.5516e+001	-1.0996e+001	-8.8264e+000	-1.5884e+001	-1.1621e+001	-1.2959e+001
6.4633e+000	3.1364e+001	-2.8253e+001	-2.0023e+001	-1.6072e+001	-2.8922e+001	-2.1161e+001	-2.3597e+001
-2.0052e+000	-9.7303e+000	8.7652e+000	6.2119e+000	4.9861e+000	8.9725e+000	6.5647e+000	7.3207e+000
5.2304e+000	2.5381e+001	-2.2864e+001	-1.6204e+001	-1.3006e+001	-2.3404e+001	-1.7124e+001	-1.9096e+001

Columns 9 through 16

1.0267e+002	-9.4504e+001	2.9238e+001	4.7436e+001	-8.0532e+000	1.1078e+000	-1.8725e+001	1.1244e+001
3.8433e+001	6.7437e+001	-6.6816e+001	-8.7840e+001	9.1333e+000	-1.4633e+000	2.6939e+001	-1.4006e+001
-1.7957e+002	2.9640e+002	-4.5288e+001	-1.3302e+002	2.1341e+001	8.0199e+000	6.6000e+001	-1.6576e+001
-4.4484e+002	-1.0564e+002	-8.6682e+001	3.8881e+001	5.3206e+000	-3.7529e+001	-5.4657e+001	-4.9637e+001
5.3591e+002	-2.9436e+002	8.2533e+001	2.2476e+002	-4.9259e+001	-1.8905e+000	-5.9613e+001	4.7354e+001
1.2945e+003	-2.8230e+002	3.7301e+002	8.7712e+001	-1.2264e+001	8.9396e+001	1.5665e+001	1.3724e+002
1.1445e+003	2.8510e+001	1.1486e+002	5.8120e+001	-3.9202e+001	4.4744e+001	5.9658e+001	8.7253e+001
6.1845e+002	-7.4721e+002	-4.9347e+001	3.7877e+002	-7.1617e+001	-6.1168e+001	-1.7097e+002	-1.5654e+000
-1.5256e+003	-1.3646e+003	-7.7002e+002	-4.9870e+002	1.4849e+002	-1.5982e+002	-1.4845e+002	-3.2420e+002
2.9499e+003	-1.9796e+003	2.3274e+003	2.1776e+003	-6.6577e+001	-3.8320e+001	-9.4739e+002	1.4040e+002
1.3772e+003	-3.0381e+003	-1.3757e+003	1.0410e+003	-2.5542e+001	-4.1779e+002	4.8778e+002	-6.9529e+002
1.3330e+003	-2.5943e+003	-3.3506e+003	-3.2616e+003	2.3896e+003	1.2332e+003	3.4207e+003	-7.1418e+002
3.0025e+002	-5.1319e+002	-6.7508e+002	-2.6277e+003	-4.0409e+002	4.7983e+002	5.1915e+002	7.7030e+000
3.0325e+002	-5.0441e+002	-6.0075e+002	-1.9199e+003	-1.1420e+003	-5.2489e+002	1.2020e+003	-1.4682e+003
6.1921e+002	-1.0037e+003	-1.4238e+003	-3.9208e+003	-1.8988e+003	-3.0178e+003	-3.1478e+003	-2.0336e+003
-3.6899e+002	6.2775e+002	8.5736e+002	1.9461e+003	9.8020e+002	1.7304e+003	4.6258e+003	-2.8057e+003
-2.7065e+002	4.6400e+002	6.1022e+002	1.3648e+003	7.0947e+002	1.1230e+003	3.5753e+003	-3.9157e+003
-1.5073e+002	2.5377e+002	3.3803e+002	7.8387e+002	3.9547e+002	5.2441e+002	1.3339e+003	-2.5404e+003

```
 2.1823e+002 -3.7038e+002 -4.8235e+002 -1.0930e+003 -5.8211e+002 -7.4988e+002 -2.2815e+003  3.8211e+003
-9.8842e+001  1.6760e+002  2.1976e+002  4.9643e+002  2.6528e+002  3.4839e+002  1.0150e+003 -1.5625e+003
-3.9192e+001  6.6474e+001  8.7325e+001  1.9820e+002  1.0355e+002  1.3890e+002  4.0040e+002 -5.7191e+002
-7.1370e+001  1.2107e+002  1.5887e+002  3.6075e+002  1.8831e+002  2.5191e+002  7.3122e+002 -1.0558e+003
 2.2146e+001 -3.7554e+001 -4.9291e+001 -1.1189e+002 -5.8607e+001 -7.8015e+001 -2.2569e+002  3.3204e+002
-5.7765e+001  9.7962e+001  1.2851e+002  2.9206e+002  1.5246e+002  2.0278e+002  5.8828e+002 -8.7054e+002

 Columns 17 through 24
 1.4571e+000  4.9553e+000  8.4962e+000 -2.8097e+000  1.1428e+000  1.5965e+000 -4.2524e-001  2.2389e+000
-4.6614e-002 -7.5300e+000 -1.2356e+001  4.1222e+000 -1.5089e+000 -1.9965e+000  6.0864e-001 -3.4482e+000
 7.3361e+000 -1.5950e+001 -1.7073e+001  5.8201e+000 -1.7190e+000 -1.3276e+000  9.8607e-001 -6.6567e+000
-4.1860e+001  9.8334e+000 -1.9452e+001  6.2114e+000 -4.7779e+000 -1.0656e+001  4.4906e-001  2.4668e+000
 1.6058e+001  1.4854e+001  3.3912e+001 -1.7328e+001  4.2364e+000  8.4183e+000 -3.6882e-001  9.1542e+000
 7.1639e+001  7.4340e+000  7.3682e+001 -1.4992e+001  1.4436e+001  2.4401e+001 -4.5375e+000  3.9371e+000
 6.9711e+001 -1.0687e+001  3.9684e+001 -1.9571e+001  7.8674e+000  1.9086e+001  1.8426e-001  5.1583e-001
-3.5817e+001  3.6156e+001  2.1356e+001 -1.7517e+001 -8.0581e-001 -2.9153e+000  3.3131e-001  1.7339e+001
-2.3569e+002  1.9526e+001 -1.6057e+002  7.5780e+001 -2.9841e+001 -6.8947e+001  5.6169e-001 -9.5768e+000
-2.2100e+002  2.5168e+002  2.1858e+002 -2.7223e+001  2.1520e+001 -6.0450e+000 -2.2978e+001  8.8356e+001
-1.7221e+002 -1.6532e+002 -4.0804e+002 -1.5957e+000 -7.9105e+001 -8.9492e+001  4.4947e+001 -3.7334e+001
 1.3818e+002 -5.9710e+002 -6.0375e+002  3.4786e+002 -4.4379e+001 -6.0400e+001  8.0285e+000 -2.8350e+002
 6.2137e+001  3.1223e+001  1.9297e+002 -2.5108e+002  3.4918e+000  6.1581e+001  2.9152e+001  9.1983e+001
-8.3883e+002  4.3217e+001 -3.8072e+002 -5.6225e+001 -1.1279e+002 -1.7384e+002  4.7551e+001  7.0397e+001
-2.8317e+003  1.2750e+003  9.0424e+002 -1.7574e+002  4.6262e+000 -2.2048e+002 -8.6443e+001  5.3619e+002
-2.7705e+002  6.7211e+002 -3.6044e+003  8.8657e+002 -5.5729e+002 -9.9186e+002  1.5544e+002 -2.0833e+002
-2.1783e+003  4.0475e+003 -2.3391e+003  9.9418e+002 -3.5124e+002 -9.9911e+002 -5.2151e+001  3.0617e+002
-4.7292e+003 -1.1686e+003 -3.4503e+003  4.6013e+002 -9.1224e+001  2.3008e+002  1.9320e+002 -7.7281e+002
 3.9900e+003  4.6642e+003 -6.5863e+003 -1.8663e+002 -2.9611e+003 -4.0696e+003  9.6574e+002 -2.2166e+003
-1.6975e+003 -1.6254e+003  6.0700e+003 -2.4866e+003  1.9447e+003  3.5125e+003  1.7780e+002  1.8568e+003
-6.0966e+002 -5.9977e+002  3.0945e+003 -2.8504e+003 -8.6808e+002 -1.2263e+003  2.7611e+002 -1.2763e+001
-1.1112e+003 -1.1203e+003  4.9306e+003 -4.5744e+003 -2.4020e+003 -4.6476e+003 -2.7571e+003  2.7931e+003
 3.5591e+002  3.3604e+002 -1.4385e+003  1.0807e+003  8.6350e+002  4.7751e+003 -6.5209e+002 -1.4059e+003
-9.2910e+002 -8.7957e+002  3.6172e+003 -3.1040e+003 -2.5554e+003 -8.5784e+003  4.1769e+003 -8.0485e+003

Input Matrix (B)

-1.4276e+003
-4.3092e+003
 2.6854e+003
 1.2284e+003
 4.5833e+002
 6.2634e+002
 4.0404e+002
 2.8258e+002
 4.1093e+002
-3.1439e+002
-1.6658e+002
-1.7390e+002
-4.1196e+001
```

```
-4.0242e+001
-8.2999e+001
 5.0047e+001
 3.6628e+001
 2.0292e+001
-2.9365e+001
 1.3305e+001
 5.2796e+000
 9.6136e+000
-2.9825e+000
 7.7799e+000
```

Output Matrix (C)

```
  Columns 1 through 8
-4.9129e-001 -1.6777e+000  1.0106e+000  3.9960e-001  8.6711e-002  9.7787e-002  6.1177e-002  2.9745e-002
-1.2479e+003 -4.2612e+003  2.5669e+003  1.0150e+003  2.2024e+002  2.4837e+002  1.5539e+002  7.5550e+001
-2.8108e-001  2.7290e-001  3.9471e-001 -2.2825e-001  2.3338e-001 -2.3788e-001  7.4759e-002 -3.0164e-001
-6.7536e+002  6.0997e+002  6.4865e+002  2.9193e+002 -3.7245e+002 -4.4630e+002 -2.3322e+002 -1.4993e+002
-8.6724e+001  1.0737e+002  2.4428e+002 -3.5595e+002  9.7773e+001  5.3946e+001  2.4164e+002 -3.1978e+001
-1.3163e+002  1.6654e+002  3.7686e+002 -5.1661e+002 -1.1523e+002  3.5849e+002  1.6224e+002 -2.2504e+002

  Columns 9 through 16
 2.3492e-002 -9.7919e-003 -2.9974e-003 -1.6594e-003 -3.0512e-004 -1.3268e-004 -3.3815e-004  1.1797e-004
 5.9669e+001 -2.4871e+001 -7.6131e+000 -4.2148e+000 -7.7497e-001 -3.3699e-001 -8.5889e-001  2.9964e-001
 2.3305e-001 -4.5770e-002  1.5725e-001 -3.6590e-002  1.1981e-001 -8.6710e-002 -2.0731e-002  2.2772e-002
 2.9429e+002 -2.1017e+002  1.1318e+002  1.3377e+002 -2.2327e+001  1.1250e+001 -4.0763e+001  4.1184e+001
-2.3902e+002 -1.9997e+002  7.5933e+001  5.9008e+000  2.4412e+001  2.4104e+000 -4.9661e+001 -8.2561e+000
-1.4686e+002 -1.1859e+002 -9.5477e+001  1.1088e+002 -2.4536e+001 -3.8560e+001 -5.2538e+001 -2.7209e+001

  Columns 17 through 24
 6.8441e-005  2.7959e-005 -2.5544e-005  8.5529e-006  3.7700e-006  3.0568e-006 -1.0090e-006  1.7143e-006
 1.7384e-001  7.1015e-002 -6.4881e-002  2.1724e-002  9.5755e-003  7.7642e-003 -2.5627e-003  4.3542e-003
 1.3494e-002 -4.6046e-003 -9.3297e-003 -2.7860e-002  2.0338e-002  1.2140e-002  3.5371e-002  1.2570e-002
 1.2048e+001  1.2001e+001  2.8103e+001 -9.1997e+000  4.1764e+000  6.6179e+000 -1.3015e+000  5.8491e+000
-2.6093e+001  1.3982e+001  2.4720e+000  8.7093e+000  2.1247e-001 -4.5938e+000 -2.3106e+000  2.1123e+000
-2.2707e+001  8.4996e+000 -8.1497e+000 -4.0674e+000 -3.2226e+000 -5.2461e+000  1.3643e+000  4.6745e+000
```

Input/Output Matrix (D)

```
     0
     0
     0
     0
     0
     0
```

8.3.3 Example #3: Upstream Static Temperature Perturbation

System Matrix (A)

Columns 1 through 7

-5.4773e+002	-9.4765e+002	-1.3159e+003	2.8145e+002	-6.3871e+001	1.3791e+001	-2.0167e+001
-2.6103e+003	-7.4443e+003	-3.4949e+003	1.3893e+003	9.3811e+002	4.9269e+002	-1.6523e+002
-1.3557e+003	-6.5274e+003	-3.9777e+003	2.7234e+002	-3.0838e+002	7.2441e+001	-3.4407e+001
5.9850e+002	2.5589e+003	2.6306e+003	-8.3260e+002	3.8044e+002	5.9080e+002	1.3443e+002
5.2505e+002	2.2312e+003	2.2510e+003	-1.4716e+003	-1.0623e+003	1.5501e+002	-2.0183e+002
3.7386e+002	1.6742e+003	1.5539e+003	-1.1411e+003	-1.6532e+003	-7.5777e+002	-1.1342e+003
-1.6627e+002	-7.6274e+002	-6.9555e+002	3.8866e+002	7.7891e+002	1.3802e+003	-2.4303e+002
3.2355e+002	1.5186e+003	1.3457e+003	-7.8775e+002	-1.6336e+003	-1.7427e+003	1.1916e+003
-4.3941e+001	-2.0411e+002	-1.8335e+002	1.1107e+002	1.8182e+002	1.8400e+002	-1.1404e+002
-1.9198e+002	-8.9445e+002	-7.9997e+002	4.9170e+002	8.1526e+002	7.5966e+002	-6.0394e+002
-1.4282e+002	-6.6117e+002	-5.9790e+002	3.5613e+002	5.7116e+002	5.6137e+002	-4.2487e+002
-9.7117e+001	-4.5023e+002	-4.0647e+002	2.4138e+002	3.9496e+002	3.9499e+002	-2.7419e+002
-2.5980e+001	-1.2052e+002	-1.0869e+002	6.4751e+001	1.0640e+002	1.0484e+002	-7.6203e+001
-5.1688e+001	-2.3991e+002	-2.1616e+002	1.2923e+002	2.1241e+002	2.0802e+002	-1.5136e+002

Columns 8 through 14

1.4456e+002	-6.8322e+000	-6.1649e+001	5.4764e+001	2.8594e+001	5.0502e+000	-1.1444e+001
-1.5585e+001	-1.1330e+001	2.8963e+001	-1.0508e+002	-5.5777e+001	-9.0842e+000	1.4878e+001
3.8080e+002	-2.4783e+001	-2.2621e+002	1.5357e+002	9.9293e+001	1.7073e+001	-4.6838e+001
-2.8405e+002	-1.9611e+001	-2.4942e+002	-1.2418e+001	1.0480e+002	1.6941e+001	-7.6210e+001
1.3603e+003	-8.5881e+000	-2.6617e+002	4.3499e+002	1.9295e+002	2.0814e+001	-4.2098e+001
1.4466e+003	-3.5453e+001	1.4964e+002	3.3832e+002	-1.1570e+002	9.9524e+000	1.1217e+002
-5.1514e+002	-5.0673e+001	2.1878e+002	1.4914e+002	-2.0211e+002	3.5562e+001	9.3667e+001
-1.9820e+003	-6.6605e+002	-1.5101e+003	-1.4721e+003	-3.8181e+002	5.2670e+000	-1.1919e+002
9.2321e+002	-6.1421e+001	1.5833e+002	3.1780e+002	-2.1233e+000	7.4723e+001	-1.9082e+001
2.9877e+003	-6.5447e+002	-1.5888e+003	2.2868e+003	1.4551e+003	3.7724e+002	-6.9642e+002
1.9517e+003	-4.8029e+002	-3.1548e+003	-2.4811e+003	1.0785e+003	-3.7628e+002	6.7691e+002
1.2074e+003	-2.7044e+002	-1.8763e+003	-3.9587e+003	-2.1315e+003	7.0014e+002	3.1153e+003
3.1452e+002	-7.8220e+001	-4.6781e+002	-7.9188e+002	-1.5270e+003	-2.7676e+002	1.6835e+003
6.2968e+002	-1.4331e+002	-8.0894e+002	-1.9200e+003	-3.3051e+003	-2.1153e+003	-1.8207e+003

```
Input Matrix (B)

  8.1786e+001
  2.3953e+002
  1.4200e+002
 -4.9812e+001
 -3.8651e+001
 -2.7999e+001
  1.2493e+001
 -2.4422e+001
  3.2879e+000
  1.4382e+001
  1.0647e+001
  7.2464e+000
  1.9392e+000
  3.8595e+000

Output Matrix (C)

   Columns 1 through 7
 -2.9112e-002 -9.5164e-002 -5.3691e-002  1.5234e-002  6.8405e-003  4.0390e-003 -1.3664e-003
 -7.2484e+001 -2.3695e+002 -1.3368e+002  3.7930e+001  1.7032e+001  1.0057e+001 -3.4021e+000
 -1.7623e-002  1.7052e-002 -2.7285e-002 -2.6338e-002  7.5828e-003 -1.4665e-002  4.7672e-003
 -3.7467e+001  3.4465e+001 -4.5170e+001  1.1039e+000 -3.4130e+001 -1.5111e+001  8.9989e-001
 -3.0526e+000  3.6306e+000 -8.5893e+000 -1.8643e+001  6.1652e+000  6.3908e+000 -4.8911e+000
 -4.6859e+000  5.6910e+000 -1.3307e+001 -2.6338e+001  9.7084e-001  2.0338e+001  1.0944e+001

   Columns 8 through 14
  1.3311e-003 -1.3864e-004 -4.2735e-004 -1.5442e-004 -6.9801e-005 -8.6634e-006 -1.8470e-005
  3.3143e+000 -3.4519e-001 -1.0640e+000 -3.8448e-001 -1.7380e-001 -2.1571e-002 -4.5987e-002
  1.0599e-002  1.2840e-002 -9.6417e-003  1.6394e-002 -1.3171e-002  1.8945e-002 -6.4994e-003
  2.0236e+001 -4.1407e-001 -6.5572e+000  9.6731e+000  4.2186e+000  7.5051e-001 -1.2412e+000
 -1.1297e+001 -3.1031e+000 -1.0465e+001  3.3443e+000  1.1321e-001  1.7666e+000 -1.5637e+000
 -6.9524e+000  9.4364e-001 -7.2950e+000 -2.9091e+000  5.8882e+000 -2.7497e-001 -3.3027e+000

Input/Output Matrix (D)

     0
     0
     0
     0
     0
     0
```

8.3.4 Example #4: Downstream Bypass Massflow Perturbation

System Matrix (A)

Columns 1 through 7

-7.2862e+001	-1.4816e+001	-6.5808e+001	7.2293e+001	-8.4572e+001	-1.3995e+001	-3.2289e+001
1.8181e+002	-3.5460e+002	-5.0998e+002	-2.7581e+001	2.0946e+002	-2.5843e+002	1.0611e+002
-7.3747e+001	7.2077e+002	-1.2157e+002	8.8203e+001	-3.4760e+002	-2.9102e+001	-9.3185e+001
9.1318e+001	-3.8158e+002	2.3512e+002	-3.9478e+002	1.3419e+003	-4.6850e+001	2.7816e+002
1.6798e+002	-6.8964e+002	5.3153e+002	-2.1557e+003	-1.8151e+003	-2.2296e+002	7.9013e+001
-7.9063e+001	3.3969e+002	-2.1554e+002	6.5952e+002	1.8753e+003	-8.3574e+002	-4.4442e+002
4.6237e+001	-1.8758e+002	1.3150e+002	-4.1284e+002	-1.0355e+003	1.1710e+003	-6.0045e+002
-5.4013e+001	2.1726e+002	-1.4978e+002	4.6604e+002	1.2794e+003	-1.2627e+003	1.3142e+003
-2.4991e+001	1.0060e+002	-6.9396e+001	2.0852e+002	5.3485e+002	-4.9904e+002	5.8302e+002
3.4354e+001	-1.3766e+002	9.5196e+001	-2.8288e+002	-7.4754e+002	7.0842e+002	-8.3503e+002
-4.4219e+001	1.7728e+002	-1.2221e+002	3.5964e+002	9.5240e+002	-8.9109e+002	1.1224e+003
-2.2718e+001	9.1033e+001	-6.2731e+001	1.8488e+002	4.9458e+002	-4.6397e+002	5.6963e+002
2.2121e+001	-8.8381e+001	6.1030e+001	-1.7927e+002	-4.8586e+002	4.6488e+002	-5.9050e+002
-1.7762e+001	7.1050e+001	-4.8965e+001	1.4397e+002	3.9284e+002	-3.7151e+002	4.6648e+002
-6.4156e+000	2.5663e+001	-1.7686e+001	5.2019e+001	1.4212e+002	-1.3458e+002	1.6895e+002
6.7755e+000	-2.7097e+001	1.8678e+001	-5.4946e+001	-1.5009e+002	1.4251e+002	-1.7863e+002
-8.6920e+000	3.4767e+001	-2.3965e+001	7.0566e+001	1.9263e+002	-1.8284e+002	2.2744e+002
5.0738e+000	-2.0295e+001	1.3989e+001	-4.1193e+001	-1.1250e+002	1.0672e+002	-1.3274e+002
6.0011e+000	-2.4004e+001	1.6545e+001	-4.8724e+001	-1.3308e+002	1.2628e+002	-1.5704e+002
2.4065e+000	-9.6258e+000	6.6350e+000	-1.9538e+001	-5.3367e+001	5.0650e+001	-6.2999e+001

Columns 8 through 14

2.3769e+001	1.7821e+001	-2.4182e+001	1.9343e+001	1.0197e+001	-2.1327e+000	-5.0685e+000
-8.9375e+001	-7.6519e+001	6.8924e+001	-9.9790e+001	-5.4646e+001	-3.9117e+001	4.9382e-001
4.5642e+001	4.1413e+001	-6.8860e+001	5.0870e+001	2.4058e+001	-1.5027e+001	-6.5985e+000
-3.8661e+002	-1.4264e+002	1.8415e+002	-4.6743e+001	-3.8390e+001	-3.4341e+001	7.0387e+001
-7.0278e+002	2.5614e+002	-3.4277e+002	8.4141e+002	3.7845e+002	-3.3410e+002	1.9899e+002
5.4652e+002	-1.8643e+002	1.7939e+002	-6.0736e+002	-2.9980e+002	2.2321e+001	-2.1624e+002
1.8997e+002	2.3646e+002	-3.9011e+002	2.5346e+002	2.5167e+002	1.8980e+002	-5.2240e+001
-1.6282e+003	5.0134e+002	-2.9352e+001	1.4913e+003	2.7333e+002	-8.6807e+002	5.3958e+002
-1.7982e+003	-6.0034e+002	8.2947e+002	-8.3996e+002	-4.6418e+002	-2.3589e+002	7.6101e+001
2.0833e+003	1.1954e+003	-2.0638e+003	-3.3759e+003	-3.4309e+002	7.1815e+002	-2.5179e+002
-3.0748e+003	-1.7369e+003	8.1714e+003	-4.0484e+003	-1.4388e+003	-1.5495e+002	-9.9536e+002
-1.4262e+003	-9.3714e+002	2.9419e+003	-3.1195e+003	-1.4772e+003	-9.3433e+002	-8.2389e+002
1.4373e+003	1.1122e+003	-2.9201e+003	4.1192e+003	3.4284e+003	-2.3805e+003	1.4001e+003
-1.0983e+003	-8.6154e+002	2.1730e+003	-3.0882e+003	-2.1206e+003	3.2728e+003	-3.9035e+003
-3.9615e+002	-3.0994e+002	7.6995e+002	-1.1405e+003	-8.4326e+002	1.3603e+003	-3.1564e+003
4.1739e+002	3.3111e+002	-8.3737e+002	1.2294e+003	8.8784e+002	-1.3427e+003	2.8905e+003
-5.2635e+002	-4.1582e+002	1.0375e+003	-1.5634e+003	-1.1080e+003	1.8552e+003	-3.9063e+003
3.0646e+002	2.4302e+002	-6.0551e+002	9.2083e+002	6.5310e+002	-1.1060e+003	2.2668e+003
3.6209e+002	2.8810e+002	-7.1782e+002	1.0969e+003	7.7741e+002	-1.2995e+003	2.6804e+003
1.4531e+002	1.1566e+002	-2.8847e+002	4.4059e+002	3.1301e+002	-5.2177e+002	1.0910e+003

```
 Columns 15 through 20
-2.6993e+000  2.6520e+000  5.2327e+000 -2.2282e+000 -4.1756e+000 -1.8986e+000
 3.1795e-001 -1.2905e+001 -1.2583e+001  1.8250e+001  1.4833e+001  3.8077e+000
-4.0774e+000  5.1066e+000  1.1608e+001 -4.3675e+000 -9.6485e+000 -4.2469e+000
 3.3758e+001 -4.1380e+001 -1.4243e+001  1.5676e+001  4.3212e+001  1.7357e+001
 5.2117e+001 -7.2879e+001  1.5452e+002 -3.9221e+001 -4.2099e+000  5.6679e-001
-7.1597e+001  1.7746e+001 -5.0789e+001  6.6667e+001  1.5164e+001 -1.2011e+001
-6.7044e+001  1.1775e+002  6.4778e+001 -7.7883e+001 -1.1734e+002 -3.5564e+001
 3.1551e+002 -4.0479e+002  1.3699e+002  7.0744e+001  2.9386e+002  9.3850e+001
 1.9980e+001 -1.4376e+002 -2.4859e+002  2.0980e+002  2.3255e+002  7.6607e+001
 2.4482e+001  3.6874e+002  3.9867e+002 -4.1975e+002 -5.7059e+002 -1.8299e+002
-3.6273e+002  1.7189e+002 -1.1994e+003  6.3827e+002  3.1396e+002  5.5860e+001
 6.2705e+001 -6.2869e+001 -6.8272e+002  3.6875e+002  2.8610e+002  1.3584e+001
 9.1123e+001 -6.9508e+002  2.7315e+002  4.2581e+002  3.8322e+002  2.3151e+002
 5.8178e+002  2.0660e+002  5.9344e+002 -4.4413e+002 -8.2435e+002 -8.0448e+002
-8.8023e+002 -4.1039e+002  3.0948e+002  4.0665e+001 -8.5235e+002 -3.3082e+002
 2.1594e+003 -1.3418e+003 -2.8785e+002  1.1679e+003  2.3287e+003  7.4790e+002
-2.4627e+003  3.5414e+003 -6.4221e+003  1.2663e+002 -2.3012e+003  2.5092e+002
 1.3863e+003 -2.2390e+003  7.4253e+003 -3.8285e+003  1.9901e+001 -3.2729e+002
 1.7234e+003 -2.6635e+003  9.6920e+003 -9.0690e+003 -8.5490e+003  6.3525e+001
 6.8404e+002 -1.0264e+003  3.4846e+003 -3.4685e+003 -6.9072e+003 -1.7264e+003

Input Matrix (B)

-1.9921e+002
 2.4238e+002
-1.2056e+002
 1.3296e+002
 2.2378e+002
-1.0858e+002
 6.2677e+001
-7.3639e+001
-3.4077e+001
 4.6898e+001
-6.0404e+001
-3.1039e+001
 3.0237e+001
-2.4283e+001
-8.7709e+000
 9.2627e+000
-1.1882e+001
 6.9360e+000
 8.2036e+000
 3.2898e+000
```

```
Output Matrix (C)

  Columns 1 through 6
  1.0508e+002   1.3254e+002   6.1244e+001  -6.2375e+001   5.4539e+001   6.9725e+001
  6.5452e+001   7.1354e+001   6.8246e+001   5.3923e+000   2.5375e+001   3.9585e+001
  8.6112e+001  -1.0746e+002   1.8288e+001  -7.0592e+001  -3.4428e+001   1.5244e+001
  7.9934e+001  -9.1433e+001   4.8431e+001  -8.8158e+001  -5.8928e+001   3.9700e+000
  6.7608e+001  -8.0561e+001   3.2624e+001   6.6782e-001   1.3859e+002  -3.4581e+001
  7.7352e+001  -9.8457e+001   4.8813e+001  -3.1675e+001   1.5032e+002  -6.2580e+001

  Columns 7 through 12
 -1.0324e+001  -3.8144e+000  -8.8503e-001   6.9272e+000   5.3348e+000   3.9267e+000
  3.3556e+001   2.1725e+000   4.0676e+000   2.9492e+000   1.9278e+000  -2.6701e-001
  3.2610e+001  -4.7076e+001  -8.9585e+000  -2.9999e+000   2.7008e+000  -7.2493e+000
  2.8337e+001  -4.6164e+001  -1.8323e+001   3.2772e+001   6.1960e-002   3.8630e+000
  3.6617e+000   3.1771e+001  -1.6422e+001   1.6443e+001  -3.9655e+001  -1.0309e+001
  2.8566e+001  -6.8316e+000  -2.1407e+001   2.8096e+001  -4.5130e+001  -2.7824e+001

  Columns 13 through 18
  1.4917e+001   5.8387e+000   3.1386e+000   9.3332e-001  -2.1558e+000  -2.6867e+000
  1.2347e+000  -3.8888e-002   4.5765e-001  -2.1187e-001  -9.8596e-001  -5.6599e-001
 -1.4954e+001   1.0568e+001   7.0605e+000  -4.9614e+000  -3.3612e+000   1.9324e+000
 -1.3636e+001   1.1599e+001   8.6036e-001  -7.0366e+000   1.8270e+000   3.4467e+000
  1.4777e-001   3.8576e+000  -4.0162e+000   3.2453e+000  -1.0327e+001   4.3481e+000
  1.6754e+001  -1.7160e+001  -3.8295e-001  -4.6959e-001  -3.7780e+000   2.4594e+000

  Columns 19 through 20
  6.5017e-001   1.0548e+000
 -1.8077e-001   1.7565e-001
  3.3582e+000   1.5588e+000
  6.5039e+000   2.4727e+000
 -1.4738e-001   1.0595e+000
  3.6392e+000  -1.1375e-001


Input/Output Matrix (D)

     0
     0
     0
     0
     0
     0
```

8.3.5 Example #5: Throat Bleed Massflow Perturbation

System Matrix (A)

Columns 1 through 7

-1.2204e+002	-1.6674e+002	-5.3600e+001	-1.5762e+002	1.2908e+002	-1.5879e+001	2.6862e+001
2.4579e+002	-1.9953e+002	5.3049e+002	1.0684e+003	-2.2272e+001	-2.6847e+002	1.8565e+002
8.7804e+001	-5.9804e+002	-3.5368e+001	2.8981e+002	-5.1233e+001	1.6739e+002	-9.2451e+000
3.0860e+002	-1.2971e+003	-4.9909e+002	-6.2832e+002	-1.6598e+003	1.2601e+003	2.9168e+002
-2.4681e+002	4.9802e+002	2.4949e+002	2.0492e+003	-7.4911e+002	-6.3801e+002	5.3221e+001
2.0504e+002	-3.6763e+002	-2.5149e+002	-1.4227e+003	1.7417e+003	-9.3524e+002	2.4437e+003
1.1931e+002	-2.9374e+002	-1.1724e+002	-6.4234e+002	7.6960e+002	-2.8925e+003	-4.5408e+002
1.0570e+002	-2.5305e+002	-1.1001e+002	-4.9303e+002	8.5180e+002	-1.5161e+003	-1.0880e+003
5.5624e+001	-1.1942e+002	-5.0725e+001	-2.3577e+002	3.5317e+002	-6.6089e+002	-4.9133e+002
-1.7507e+002	3.6924e+002	1.7001e+002	7.5028e+002	-1.2896e+003	1.8527e+003	1.9039e+003
6.4549e+001	-1.4112e+002	-6.3791e+001	-2.8150e+002	4.5278e+002	-6.9615e+002	-5.5533e+002
-1.1479e+002	2.5023e+002	1.1513e+002	5.4683e+002	-7.7736e+002	1.0614e+003	8.4778e+002
3.7112e+001	-8.0129e+001	-3.7309e+001	-1.7424e+002	2.4642e+002	-3.4164e+002	-2.7362e+002
-5.5600e+001	1.1803e+002	5.5511e+001	2.6084e+002	-3.6792e+002	4.9090e+002	4.3914e+002
4.5360e+001	-9.6161e+001	-4.4624e+001	-2.1089e+002	2.9555e+002	-4.0593e+002	-3.5103e+002
-3.8666e+001	8.2981e+001	3.7949e+001	1.7863e+002	-2.5283e+002	3.5965e+002	2.8697e+002
5.4859e+001	-1.1742e+002	-5.3869e+001	-2.5375e+002	3.5775e+002	-5.0664e+002	-4.0866e+002
-2.0626e+001	4.4168e+001	2.0272e+001	9.5502e+001	-1.3500e+002	1.9038e+002	1.5390e+002
2.1151e+001	-4.5258e+001	-2.0834e+001	-9.8241e+001	1.3844e+002	-1.9365e+002	-1.5862e+002
-2.7123e+001	5.8042e+001	2.6726e+001	1.2594e+002	-1.7770e+002	2.4842e+002	2.0375e+002
1.3175e+001	-2.8224e+001	-1.2983e+001	-6.1173e+001	8.6412e+001	-1.2100e+002	-9.8666e+001
2.2703e+001	-4.8629e+001	-2.2375e+001	-1.0538e+002	1.4895e+002	-2.0854e+002	-1.7014e+002
-1.2916e+001	2.7666e+001	1.2725e+001	5.9919e+001	-8.4728e+001	1.1873e+002	9.6789e+001
2.1458e+001	-4.5955e+001	-2.1141e+001	-9.9535e+001	1.4080e+002	-1.9719e+002	-1.6100e+002
-8.8465e+000	1.8944e+001	8.7156e+000	4.1036e+001	-5.8038e+001	8.1279e+001	6.6369e+001
-4.1125e+000	8.8071e+000	4.0518e+000	1.9078e+001	-2.6979e+001	3.7783e+001	3.0846e+001

Columns 8 through 14

6.5572e+001	-2.6498e+001	6.9850e+001	-1.0315e+001	-1.1142e+002	2.4570e+001	-5.2243e+000
1.7566e+002	2.3695e+001	2.9961e+001	6.2509e+001	-8.8871e+001	1.7967e+001	7.8702e+001
2.2332e+001	-3.0769e+001	9.8031e+000	6.1656e+000	-3.4738e+001	2.7881e+001	-4.3008e+001
-5.7389e+001	-1.3939e+002	5.3258e+002	-2.1571e+002	-2.5567e+002	5.1053e+001	-1.3599e+002
-4.7453e+002	2.8140e+001	8.9557e+002	-2.3135e+002	2.8033e+002	-4.3904e+001	8.7873e+001
1.1185e+003	4.5342e+002	-9.7275e+002	5.0433e+002	2.4234e+001	-1.0581e+001	3.7128e+002
4.3043e+002	1.6859e+002	-1.6456e+003	2.5440e+002	1.5164e+002	-6.1401e+001	-2.9456e+002
-5.7127e+002	5.7596e+002	-2.0115e+003	-8.3627e+001	3.8441e+002	-1.4893e+002	-3.1772e+002
-1.0079e+003	-1.9490e+002	-1.5954e+003	2.8668e+001	-7.0129e+002	1.5540e+002	-3.5242e+002
2.9831e+003	2.4603e+003	-2.5383e+003	-1.4404e+003	3.2243e+003	-7.8533e+002	1.7060e+002
-6.4046e+002	-4.7503e+002	3.0060e+003	-4.4910e+002	-1.7316e+003	1.2144e+002	-5.0130e+002
1.1374e+003	1.0248e+003	-4.5921e+003	2.4449e+003	-3.0384e+003	-6.7270e+002	1.7871e+003
-3.7016e+002	-2.9645e+002	1.2969e+003	-5.6100e+002	2.4284e+003	-4.4791e+002	-1.7516e+003
6.2305e+002	4.5078e+002	-1.6634e+003	9.0706e+002	-3.8926e+003	2.6950e+003	-1.2872e+003
-5.1023e+002	-3.3171e+002	1.2989e+003	-7.0332e+002	3.1531e+003	-1.8814e+003	2.2144e+003
4.0168e+002	2.6454e+002	-1.1424e+003	5.1673e+002	-2.2449e+003	1.0673e+003	-2.6234e+003

```
-5.8232e+002 -3.8072e+002  1.6093e+003 -7.5407e+002  3.2640e+003 -1.4901e+003  3.1579e+003
 2.1907e+002  1.4539e+002 -6.0016e+002  2.8920e+002 -1.1433e+003  5.3535e+002 -1.0819e+003
-2.2444e+002 -1.5117e+002  6.2519e+002 -3.0022e+002  1.1238e+003 -5.2431e+002  9.5974e+002
 2.8737e+002  1.9392e+002 -7.9868e+002  3.8233e+002 -1.4420e+003  6.6630e+002 -1.2147e+003
-1.3885e+002 -9.4226e+001  3.8898e+002 -1.8532e+002  6.8205e+002 -3.1519e+002  6.1031e+002
-2.3933e+002 -1.6234e+002  6.6780e+002 -3.1848e+002  1.1799e+003 -5.3941e+002  1.0416e+003
 1.3597e+002  9.1965e+001 -3.7905e+002  1.8008e+002 -6.7683e+002  3.0904e+002 -6.0340e+002
-2.2605e+002 -1.5278e+002  6.2764e+002 -2.9927e+002  1.1258e+003 -5.1674e+002  9.9245e+002
 9.3219e+001  6.2961e+001 -2.5879e+002  1.2344e+002 -4.6477e+002  2.1290e+002 -4.0862e+002
 4.3311e+001  2.9267e+001 -1.2043e+002  5.7381e+001 -2.1560e+002  9.8642e+001 -1.9015e+002

 Columns 15 through 21
-2.5227e+001  1.2369e+001 -4.2181e+001  1.0671e+001 -7.6251e+000  9.7250e+000  5.3717e+000
-8.7031e+001 -4.7962e+001  1.5207e+001 -7.0619e+000 -2.1756e+001  2.7996e+001  9.2904e+000
 1.5140e+000  2.2278e+001 -2.8648e+001  1.3187e+001 -5.2153e-003 -6.3224e+000  2.3227e+000
 6.2512e+001  9.1611e+001 -9.0457e+001  3.7293e+001  7.1989e+001 -8.2440e+001  4.4465e+001
 6.3292e+001 -5.7457e+001  1.9320e+002 -3.8944e+001  8.5190e+001 -6.7704e+001  1.1684e+001
-2.7820e+002 -2.5198e+002  2.2138e+002 -9.9944e+001 -1.2204e+002  1.5948e+002 -1.8405e+001
 2.3102e+002  1.1442e+002 -1.2264e+002  5.4808e+001  1.6232e+000 -5.6220e+001 -4.0510e+001
 4.2866e+002  1.3721e+002  1.6342e+002 -9.0207e+001  1.5091e+002 -1.7507e+002  7.3656e+000
 9.2173e+001  1.9749e+002 -2.2486e+002  4.6194e+001  4.8195e+001 -7.5009e+001  5.7439e+001
 1.9893e+002  1.5788e+002 -8.5667e+001 -9.6399e+001 -3.1129e+002  2.7480e+002 -2.9310e+002
 4.1171e+002  2.5719e+002 -1.5873e+002 -3.0778e+001  2.0494e+002 -1.7696e+002  1.0184e+002
-2.1451e+003  1.1785e+003 -2.7151e+003  6.2794e+002 -2.7240e+002  4.1777e+002  3.2503e+002
 1.5384e+003 -5.2808e+002  8.4958e+002 -2.8582e+002  2.1773e+002 -2.2441e+002 -3.7285e+001
-1.7889e+002  2.4707e+003 -2.3692e+003  7.1133e+002  2.0023e+002 -4.8649e+002 -9.4093e+000
-1.2824e+003 -3.0203e+003  1.6307e+003 -3.7706e+002 -5.6501e+002  7.6846e+002  2.0909e+002
 3.7239e+003 -1.8385e+003 -3.3676e+002  4.7560e+002 -9.5283e+002  1.2093e+003 -2.8779e+002
-3.7479e+003  5.4761e+003 -4.7630e+003  7.7830e+001  7.4546e+002 -1.1931e+003  8.5909e+002
 1.2697e+003 -2.2144e+003  3.5303e+003 -9.8495e+002 -1.6306e+003  2.4646e+003 -6.8694e+002
-1.1175e+003  2.2792e+003 -3.9449e+003  2.8808e+003 -1.9644e+003  1.1105e+003  5.6267e+001
 1.4403e+003 -2.8774e+003  5.0913e+003 -3.7307e+003  4.0649e+003 -3.6857e+003 -9.1696e+002
-7.6316e+002  1.2991e+003 -2.4646e+003  1.4627e+003 -2.4796e+003  4.1698e+003 -1.3567e+003
-1.3057e+003  2.2707e+003 -4.1831e+003  2.3202e+003 -4.3439e+003  6.6576e+003 -3.6677e+003
 7.4981e+002 -1.1943e+003  2.2027e+003 -1.2456e+003  2.5227e+003 -3.7088e+003  2.3290e+003
-1.2191e+003  2.0453e+003 -3.7655e+003  2.0641e+003 -4.1480e+003  5.9438e+003 -4.4143e+003
 5.0000e+002 -8.4625e+002  1.5395e+003 -8.3907e+002  1.6702e+003 -2.4201e+003  1.8904e+003
 2.3366e+002 -3.9218e+002  7.2007e+002 -3.9753e+002  7.7834e+002 -1.1313e+003  8.3913e+002

 Columns 22 through 26
 1.0590e+001 -2.4664e+000  2.0753e+000  2.4740e+000 -2.8947e+000
 1.3647e+001 -2.0880e+001  2.1398e+001  1.5232e-001 -3.8347e+000
 1.0530e+001 -1.5763e+000  2.5537e+000 -1.5201e+000 -3.0766e+000
 7.0386e+001 -6.1859e+000 -2.7115e+001  1.5425e+001 -8.4221e-001
-7.9240e+000  4.0208e+000 -1.1056e+002  3.6899e+001  1.6730e+001
-2.7914e+001 -5.6274e+001  8.6491e+001 -2.0243e+001 -4.5675e+000
-5.6761e+001  4.6772e+001  6.5658e+001 -4.0798e+001 -1.1941e+000
 3.3886e+001  3.2060e+001  9.4838e+000 -4.1909e+001  2.5848e+001
```

```
 1.3560e+002 -1.8267e+001  5.7429e+001 -2.1075e+001 -1.3014e+001
-3.9183e+002  1.7628e+002  2.6943e+002 -1.8949e+002  1.1490e+001
 1.6141e+002  2.9841e+001 -7.0527e+001  2.2381e+001  2.1168e+001
 5.6878e+002 -7.4304e+001  4.6739e+001  1.5579e+002 -1.1560e+002
-2.1905e+002  7.6061e+001  1.0105e+002 -5.2793e+001  7.9765e+001
 2.4632e+002  2.3267e+002  5.1932e+001 -1.2941e+002 -5.1059e+001
 3.4522e+002 -4.9736e+002  1.9579e+002  1.2262e+002 -1.3326e+002
-9.9426e+002 -4.8293e+002 -9.9496e+001  2.4833e+002  8.4856e+001
 1.6561e+003  4.5792e+002  7.7133e+002 -7.7303e+001 -3.9795e+002
-7.2219e+002  8.5087e+001 -2.0377e+002 -1.8091e+002  2.3859e+002
 3.1737e+002 -4.8061e+002  1.2589e+003 -4.1073e+002 -3.9227e+002
-1.0763e+003  6.7759e+002 -7.5911e+002  2.0883e+002  3.2370e+002
-1.4317e+003  7.2591e+002 -1.9250e+001 -5.9555e+002  1.1932e+002
-5.7232e+003 -1.2454e+002  1.3250e+002 -3.1690e+002  7.0526e+002
 6.5920e+003 -2.8614e+003 -9.0516e+002  1.0092e+003 -5.0397e+002
-1.0861e+004  9.9609e+003 -1.5774e+004  4.4744e+003  5.6350e+002
 4.5117e+003 -4.1752e+003  1.0744e+004 -5.3019e+003  3.1974e+003
 2.0084e+003 -1.7506e+003  5.8865e+003 -6.7250e+003 -2.0406e+003

Input Matrix (B)

 -2.4037e+002
  1.8351e+002
  7.0707e+001
  2.6677e+002
 -2.2492e+002
  2.0050e+002
  1.1924e+002
  1.0681e+002
  5.3954e+001
 -1.7074e+002
  6.3374e+001
 -1.1403e+002
  3.6701e+001
 -5.4779e+001
  4.4588e+001
 -3.8057e+001
  5.3971e+001
 -2.0303e+001
  2.0825e+001
 -2.6706e+001
  1.2976e+001
  2.2360e+001
 -1.2719e+001
  2.1131e+001
 -8.7118e+000
 -4.0500e+000
```

```
Output Matrix (C)

  Columns 1 through 7
  3.0505e+001 -6.5875e+001 -8.7394e+000 -5.5885e+001  3.3035e+001 -4.0881e+001  4.9231e-001
  1.5579e+002  5.5421e+001  2.7211e+001 -5.3916e+001 -2.1185e+002  3.7076e+001  4.6370e+001
  6.5869e+001 -2.4503e+001 -2.2642e+001  1.3577e+002  4.9109e+001 -5.5824e+001 -3.5948e+001
  1.2068e+002 -3.7302e+001  5.2595e+001  2.1236e+002  4.2892e+001 -1.3374e+002 -1.4565e+001
  7.3142e+001  9.9222e+001 -3.0018e+001 -2.0219e+001 -4.5510e+000  6.1225e+001 -3.4094e+001
  9.1236e+001  1.2012e+002 -1.6531e+000 -3.4558e+001  1.8608e+001  1.1138e+002 -9.6961e+001

  Columns 8 through 14
 -3.8166e+001 -2.5756e+001  2.5250e+001 -7.8352e+000  1.2615e+001 -6.0444e+000 -1.2070e+000
 -3.9859e+001  2.3583e+001  7.0783e+001 -1.2150e+001  6.4873e+001 -1.1345e+001  1.6531e+001
  3.5594e+001  2.0339e+001 -5.3962e+001  5.6480e+001  5.4349e+001  8.1780e+000  2.4220e+000
 -1.8685e+001  2.9043e+001 -1.1834e+002  1.9432e+001  5.6581e+001 -2.4905e+001  2.9471e+001
 -6.5918e+001 -2.0413e+001 -5.0734e+001 -1.1715e+001  3.7915e+001  6.6175e+000 -3.2401e+001
 -4.9010e+001 -4.1983e+000 -6.3358e+001 -1.0121e+001  3.2304e+001 -2.1232e+001 -2.8316e+001

  Columns 15 through 21
 -2.3781e+000 -4.1113e+000  1.2207e+001 -2.8528e+000  8.5243e+000 -1.3199e+001  8.6559e+000
  1.1323e+001 -1.6576e+001  4.1264e+001 -7.9378e+000  1.2625e+001 -1.1570e+001  5.5765e-001
 -1.0332e+001 -1.5811e+001  1.6235e+001  4.6995e+000 -7.2824e+000  1.7956e+000 -5.4218e+000
  8.3326e-001 -1.5839e+001  2.5961e+001 -1.5061e+001 -7.3850e+000  1.1559e+001 -6.6411e+000
  2.0620e+001  2.2637e+001 -2.9667e-001 -5.5393e+000  8.9550e-001 -1.6495e+000 -4.0159e+000
  3.6354e+001  1.1974e+001 -1.1110e+001  7.8393e+000  9.6571e+000 -1.6297e+001 -1.8738e+000

  Columns 22 through 26
-4.0692e+000 -5.1593e-001  1.4963e+001 -9.5835e+000  1.4722e+001
 4.0358e+000  2.7466e+000 -3.8064e+000 -5.5925e-001 -1.3082e+001
-1.4032e+000 -1.5962e+000 -7.9722e+000 -2.6423e+000  2.9358e+000
-4.0166e+000  2.0386e+000 -1.1587e+001  2.1054e+000  6.2389e+000
-4.6068e+000  9.7055e-002  3.0720e+000  3.9048e+000 -1.5866e+000
-1.9299e+000  1.3708e+000 -7.3702e+000  6.5548e+000  2.9289e+000

Input/Output Matrix (D)

     0
     0
     0
     0
     0
     0
```

9 References

[1] G. L. Cole & R. G. Willoh, "Analysis of the Dynamic Response of a Supersonic Inlet to Flow-Field Perturbations Upstream of the Normal Shock," NASA TN D-7839, January, 1975.

[2] A. W. Martin, "Propulsion System Dynamic Simulation Theory and Equations," of North American Aviation, NASA CR-928, March, 1968.

[3] F. R. Barry, "Frequency of Supersonic Inlet Unstarts Due to Atmospheric Turbulence," of Hamilton Standard, HSER-5838, October, 1973.

[4] T. R. Stalzer & G. J. Fiedler, "Criteria for Validity of Lumped-Parameter Representation of Ducting Air-Flow Characteristics," Transactions of the ASME, pp. 833-839, 1957.

[5] A. Sarantopoulos & T. T. Hartley, "Modeling of Linear Isentropic Flow Systems," Proceedings of the IEEE International Conference on Systems Engineering, Dayton, OH, August, 1991.

[6] A. Sarantopoulos, "Development of Transfer Functions for Partial Differential Equations with Propulsion System Applications," Ph. D. Dissertation, University of Akron, Akron, OH, August, 1994.

[7] G. K. Cooper & J. R. Sirbaugh, "The PARC Code: Theory and Usage," AEDC-TR-89-15, December, 1989.

[8] M. O. Varner, et al, "Large Perturbation Flow Field Analysis and Simulation for Supersonic Inlets: Program Modifications," Sverdrup Technology, Contract NAS3-24105, April 1987.

[9] C. Hirsch, *Numerical Computation of Internal and External Flows Vol. 1 & 2,* Chinchester, Wiley, 1990.

[10] J. L. Steger & R. F. Warming, "Flux Vector Splitting of the Inviscid Gas Dynamic Equations with Application to Finite-Difference Methods," Journal of Computational Physics, vol. 40, pp. 263-293, 1981.

[11] K. V. Fernando & H. Nicholson, "Singular Perturbational Model Reduction of Balanced Systems," IEEE Transactions on Automatic Control, vol. AC-34, pp. 729-733, 1981.

[12] A. Chicatelli, "Methods for Developing Linear Reduced Models of Internal Flow Propulsion Systems," MS Thesis, University of Akron, Akron, OH, May, 1990.

[13] B. C. Moore, "Principal Component Analysis in Linear Systems: Controllability, Observability, and Model Reduction," IEEE Transactions on Automatic Control, vol. AC-26, pp. 17-32, 1981.

[14] A. J. Laub, "Computation of Balancing Transformations," Proceedings of the Joint Automatic Control Conference, San Francisco, August, 1980.

[15] L. Pernebo & L. M. Silverman, "Model Reduction via Balanced State Space Representations," IEEE Transactions on Automatic Control, vol. AC-27, pp. 382-387, 1982.

[16] M. G. Safonov & R. Y. Chiang, "A Schur Method for Balanced-Truncation Model Reductions," IEEE Transactions on Automatic Control, vol. AC-34, pp. 729-733, 1989.

[17] K. Glover, "All Optimal Hankel Norm Approximations of Linear Multivariable Systems and their L^{∞}-error Bounds, " International Journal of Control, vol. 39, pp. 1115-1139, 1984.

REPORT DOCUMENTATION PAGE

Form Approved
OMB No. 0704-0188

1. AGENCY USE ONLY (*Leave blank*)	2. REPORT DATE	3. REPORT TYPE AND DATES COVERED
	January 1997	Final Contractor Report

4. TITLE AND SUBTITLE

A Method for Generating Reduced Order Linear Models of Supersonic Inlets

5. FUNDING NUMBERS

WU-509-10-11
G-NAG3-1450

6. AUTHOR(S)

Amy Chicatelli and Tom T. Hartley

7. PERFORMING ORGANIZATION NAME(S) AND ADDRESS(ES)

University of Akron
Akron, Ohio 44325

8. PERFORMING ORGANIZATION REPORT NUMBER

E-10479

9. SPONSORING/MONITORING AGENCY NAME(S) AND ADDRESS(ES)

National Aeronautics and Space Administration
Lewis Research Center
Cleveland, Ohio 44135-3191

10. SPONSORING/MONITORING AGENCY REPORT NUMBER

NASA CR-198538

11. SUPPLEMENTARY NOTES

Project Manager, Kevin J. Melcher, Instrumentation and Controls Division, NASA Lewis Research Center, organization code 5530, (216) 433-3743.

12a. DISTRIBUTION/AVAILABILITY STATEMENT

Unclassified - Unlimited
Subject Categories 08 and 01

This publication is available from the NASA Center for AeroSpace Information, (301) 621-0390.

12b. DISTRIBUTION CODE

13. ABSTRACT (*Maximum 200 words*)

For the modeling of high speed propulsion systems, there are at least two major categories of models. One is based on computational fluid dynamics (CFD), and the other is based on design and analysis of control systems. CFD is accurate and gives a complete view of the internal flow field, but it typically has many states and runs much slower than real-time. Models based on control design typically run near real-time but do not always capture the fundamental dynamics. To provide improved control models, methods are needed that are based on CFD techniques but yield models that are small enough for control analysis and design.

14. SUBJECT TERMS	15. NUMBER OF PAGES
Inlet modeling; Linearization; CFD; Reduced order modeling; Error bounds	62
	16. PRICE CODE: A04

17. SECURITY CLASSIFICATION OF REPORT	18. SECURITY CLASSIFICATION OF THIS PAGE	19. SECURITY CLASSIFICATION OF ABSTRACT	20. LIMITATION OF ABSTRACT
Unclassified	Unclassified	Unclassified	